

GRAPHENE: ELECTRON PROPERTIES AND TRANSPORT PHENOMENA

Leonid Levitov

Massachusetts Institute of Technology

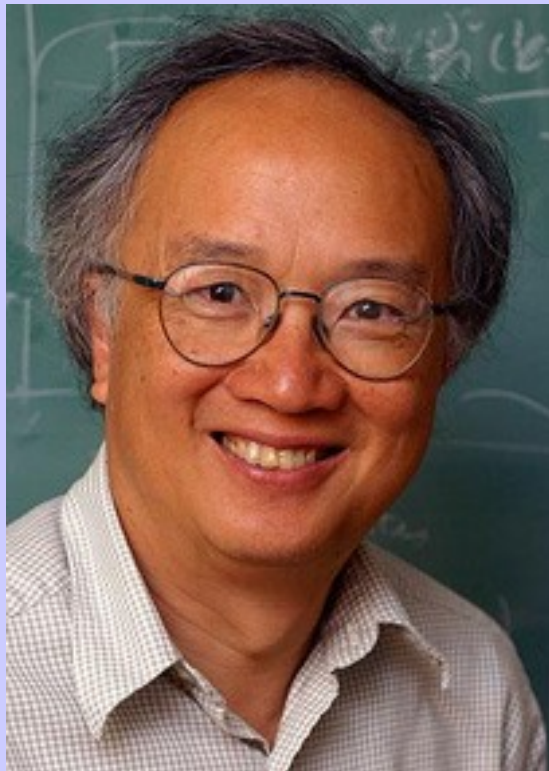
Lecture notes and HW problems:

<http://www.mit.edu/~levitov/>

Summer School, Chernogolovka 2007



Dima Abanin (MIT)



Andrey Shytov
(BNL)

Misha Katsnelson
(Nijmegen)

Patrick Lee
(MIT)



Lecture I

Background:

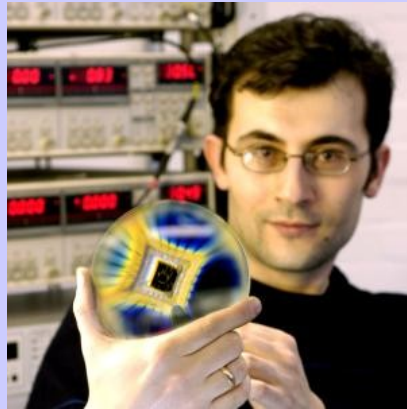
Field effect in graphene,
Quantum Hall effect,
p-n junctions

Electron transport in graphene monolayer

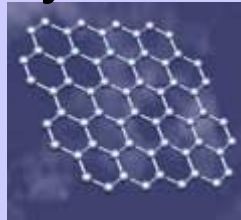
*New 2d electron system (Manchester 2004):
Nanoscale electron system with tunable properties;*



Andrey Geim



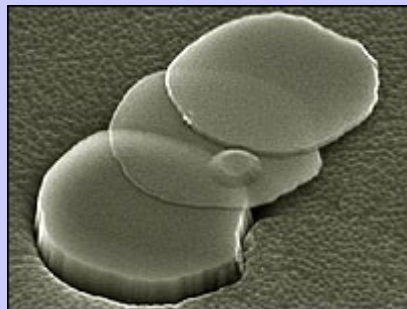
Kostya Novoselov



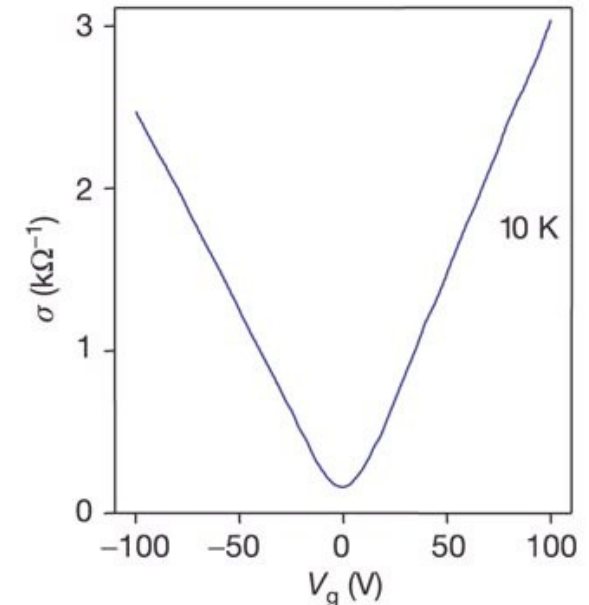
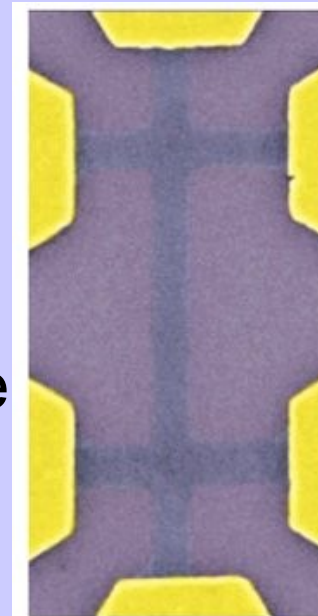
Monolayer graphene



Philip Kim



Field-effect enabled by gating:
conductivity linear in density,
mobility, density vs gate voltage



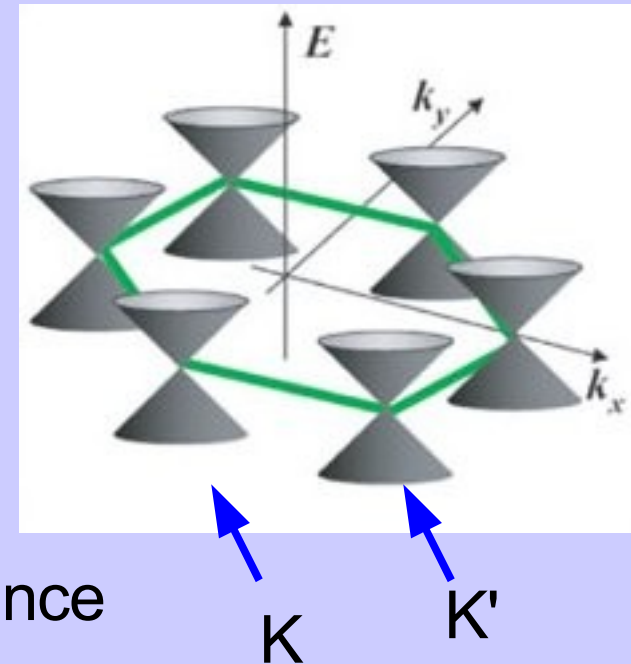
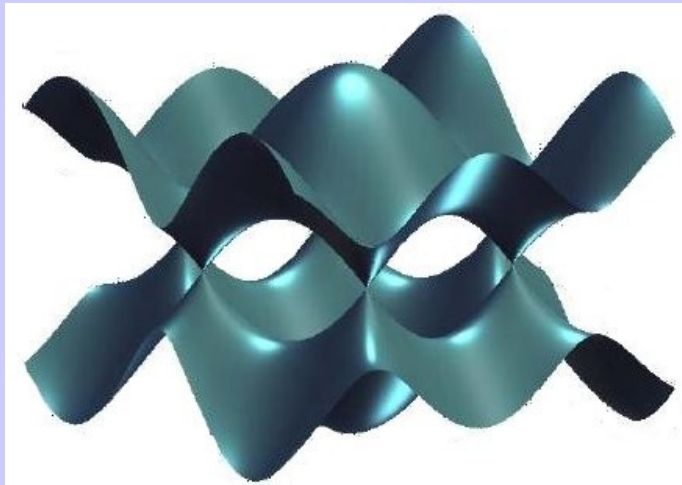
Novoselov et al, 2004, Zhang et al, 2005

Interesting Physical Properties

Semimetal (zero bandgap); electrons and holes coexist

Massless Dirac electrons, $d=2$

Graphene electron band structure,
mimic Dirac electrons at points K and K'



Manifestations: “relativistic” Lorentz invariance
with Fermi velocity instead of light speed

"Half-integer" Quantum Hall Effect

Single-layer graphene:
QHE plateaus observed at

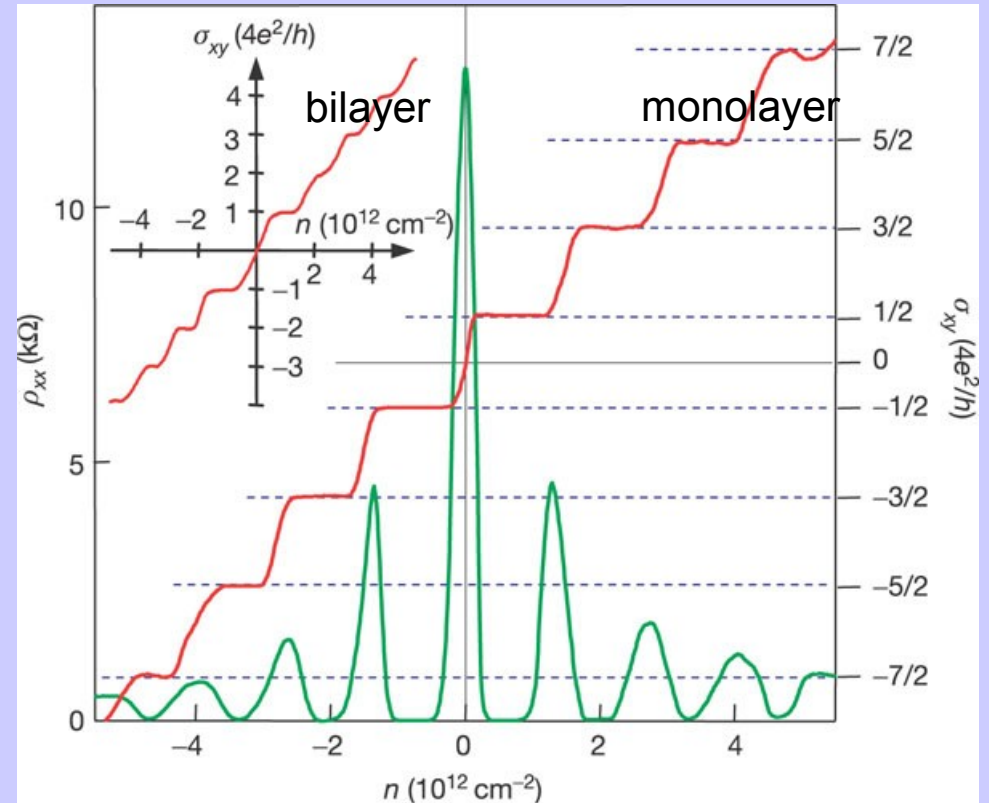
$$\nu = 4 \times (0, \pm 1/2, \pm 3/2 \dots)$$

4=2x2 spin and valley degeneracy

Manifestation of relativistic Dirac electron properties

Landau level spectrum
with very high cyclotron
energy (1000K)

Recently: QHE at T=300K



Novoselov et al, 2005, Zhang et al, 2005

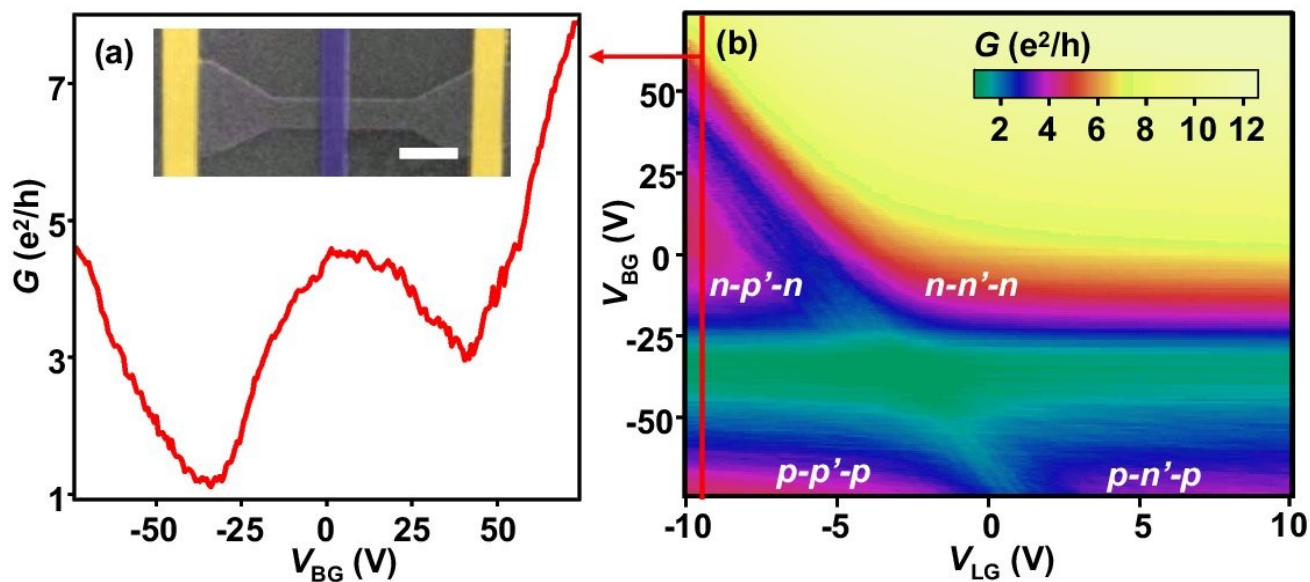
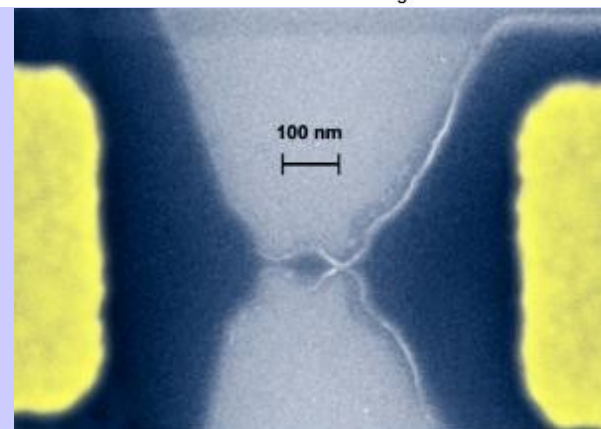
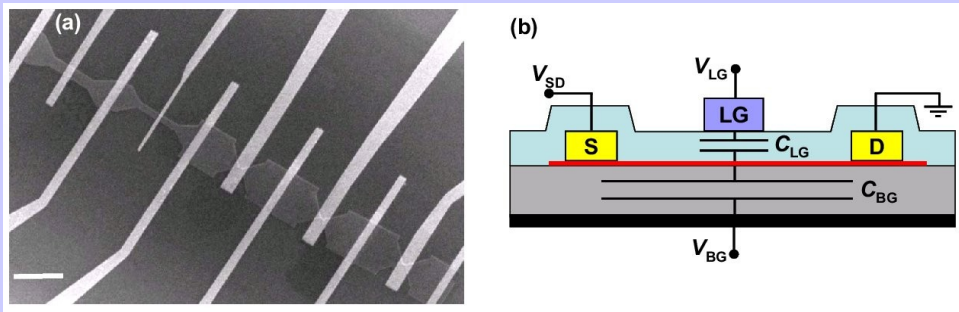
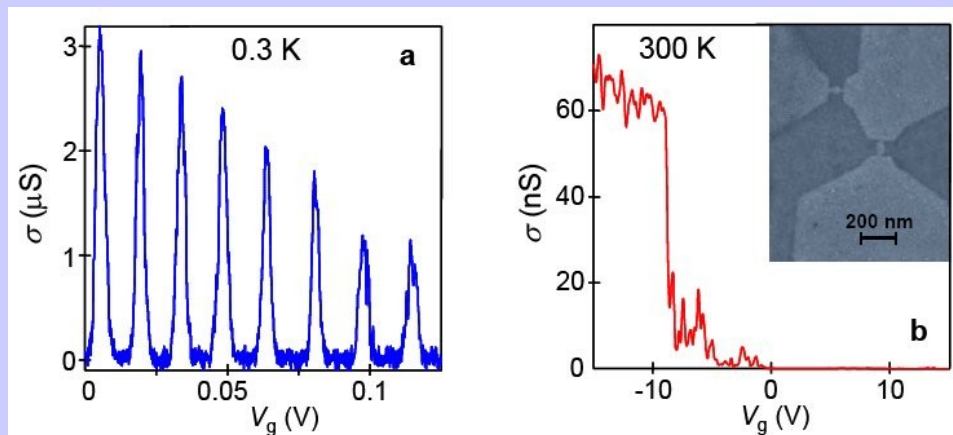
Recently: Graphene devices

Devices in patterned graphene:

quantum dots (Manchester),
nanoribbons (IBM, Columbia);

Local density control (gating):
p-n and p-n-p junctions

(Stanford, Harvard, Columbia)

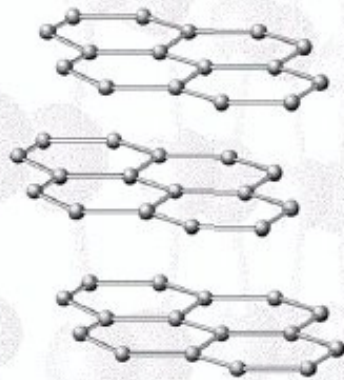


Equal or opposite polarities of charge carriers in the same system (electrons and holes coexist)

Electron properties of graphene

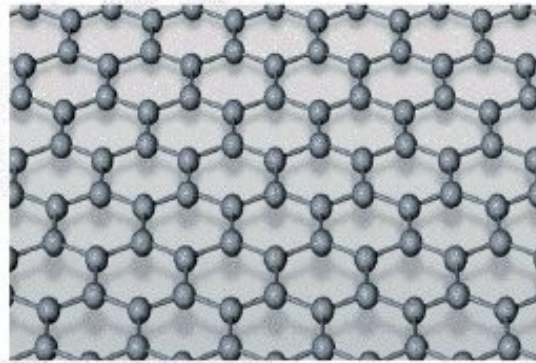
GRAPHENE ALLOTROPES

3D



Graphite

2D



graphene

PRESUMED
NOT TO EXIST
IN THE FREE STATE

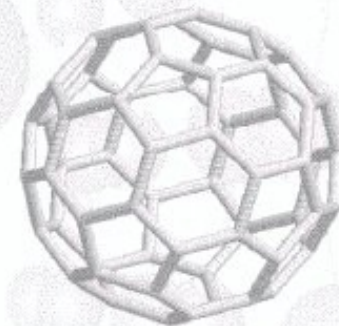
1D



*Carbon
Nanotube*

multi-wall:
1952 to Iijima 1991
single-wall: 1993

0D



Buckyballs

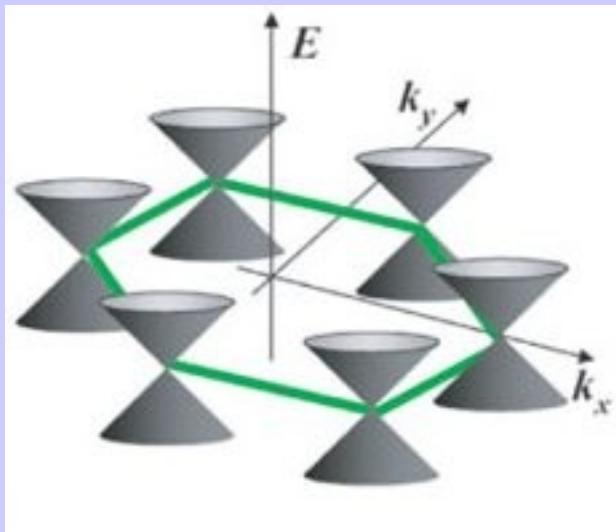
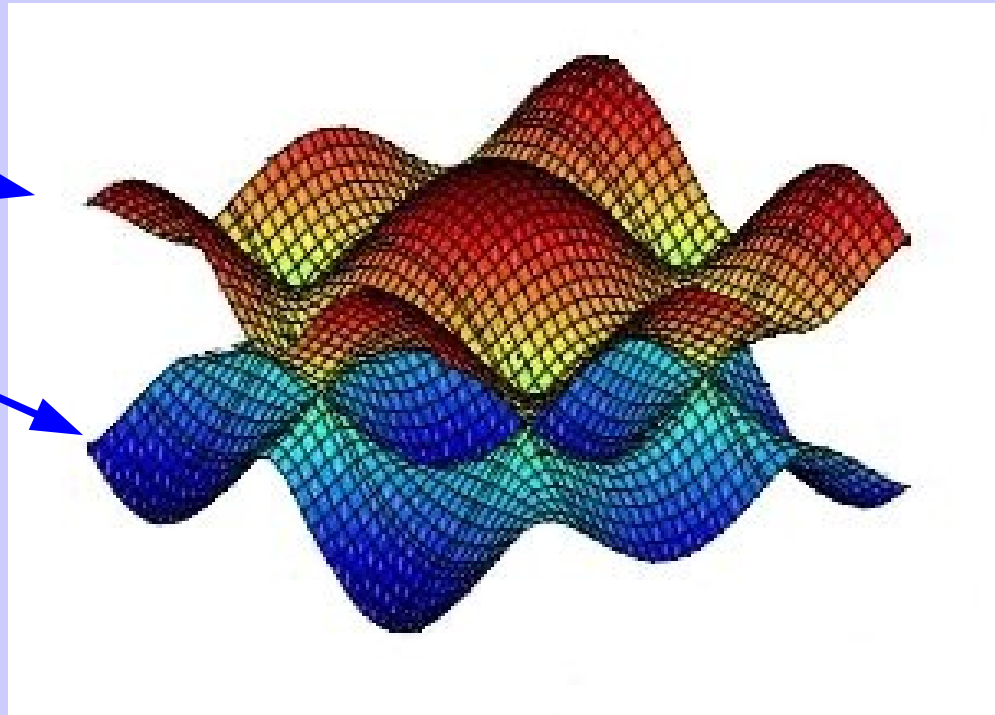
Kroto et al 1985

Tight-binding model on a honeycomb lattice

Conduction band

Valence band

Dirac model:



K K'

Velocity $v = dE/dp = 10^8 \text{ cm/s} = c/300$

Density of states linear in E,
and symmetric $N(E) = N(-E)$

Other effects: next-nearest neighbor hopping; spin-orbital coupling;
trigonal warping (ALL SMALL)

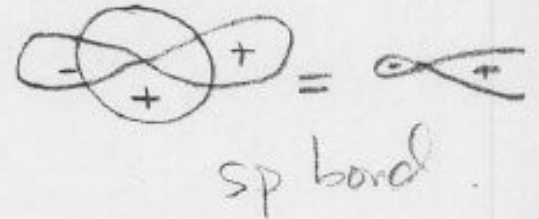
S and P electron orbitals

Carbon: 6 electrons

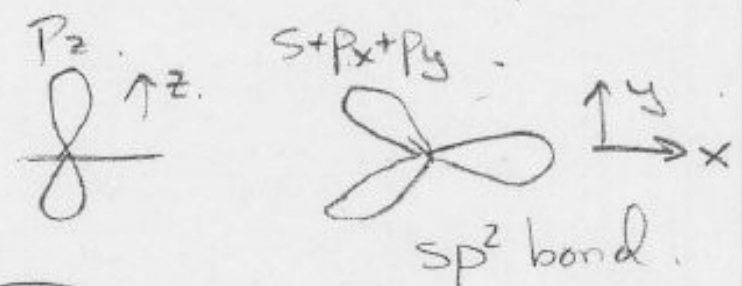
$1s^2 2s^2 2p^2$ atomic.
 $1s^2 \underbrace{2s 2p^3}_{sp \text{ bonds}}$ bonding.

Don't trust details of notes!

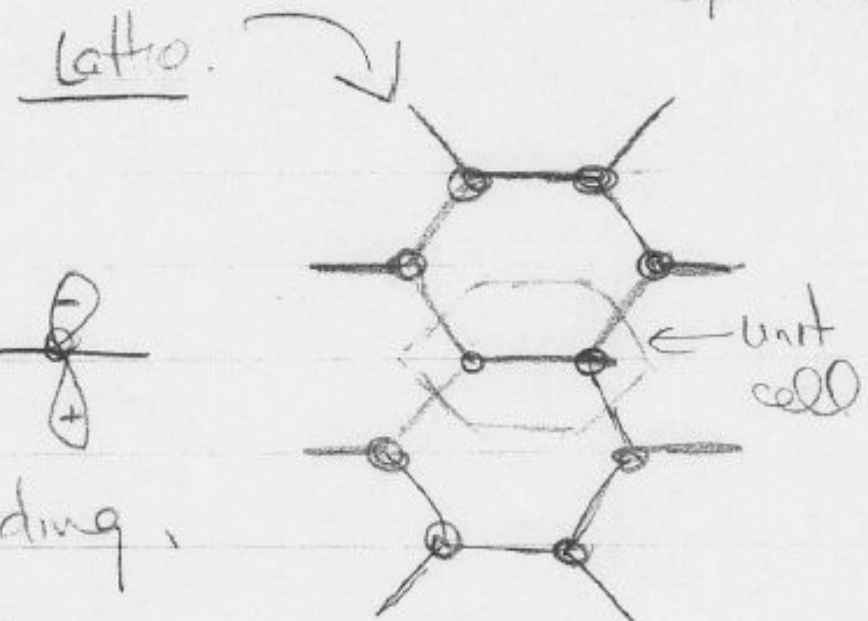
sp^2 bonds give honeycomb lattice. One p_z orbital left over per C-atom.



p_z responsible for conduction



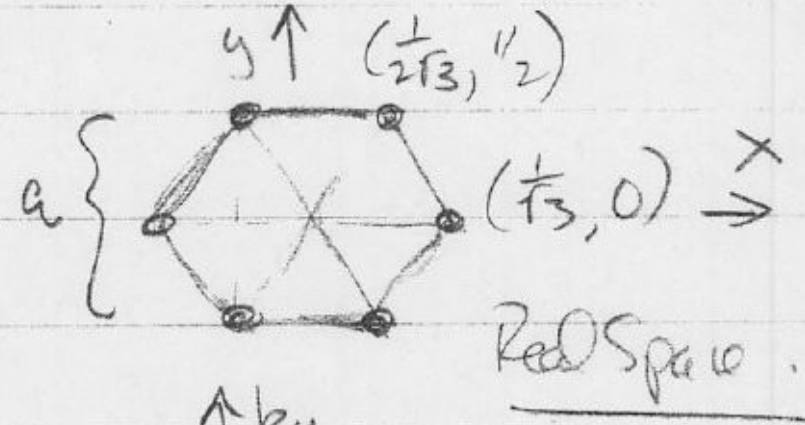
Unit cell:
 Two atom basis.
 Side view:



bonding called "pi" orbitals.
 antibonding

Real space, reciprocal space

Unit Cell. Real & Recip Space.
 Set "a" = 1. $a = \sqrt{3} \cdot c$ -c bond length.

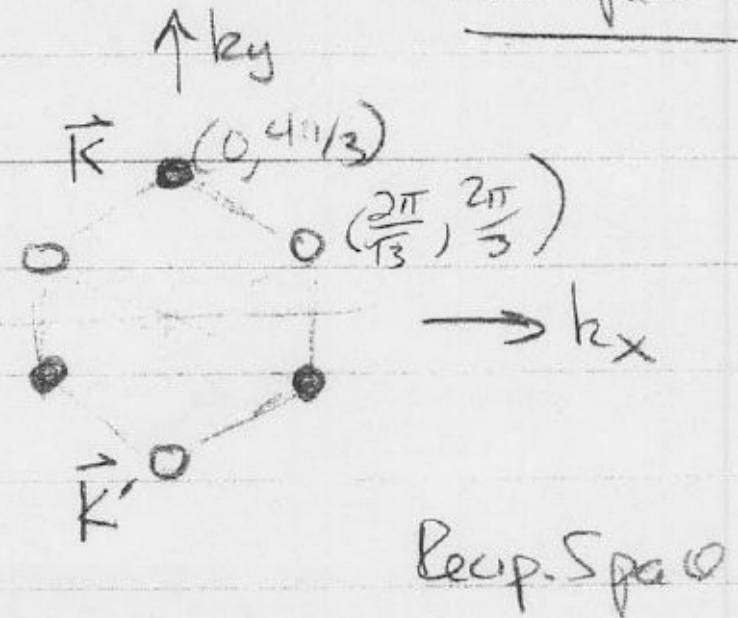


First Brillouin Zone \Rightarrow exactly filled by 2 atom lattice.

Two "special" points:

- $\vec{K} = (0, \frac{4\pi}{3})$
- $\vec{K}' = (0, -\frac{4\pi}{3})$

Note: other corners related by recip. lattice vectors.



Graphene: tight-binding model

Tight Binding Model:

Assume N-N hopping with element t .

Need two #'s to describe basis

Write as column vector.

$\begin{pmatrix} 1 \\ 0 \end{pmatrix} \Rightarrow$ electron on A,
 $\begin{pmatrix} 0 \\ 1 \end{pmatrix} \Rightarrow$ electron on B.

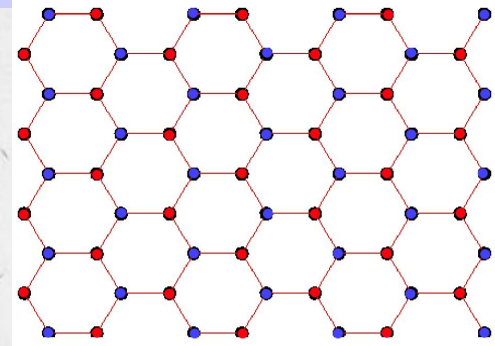
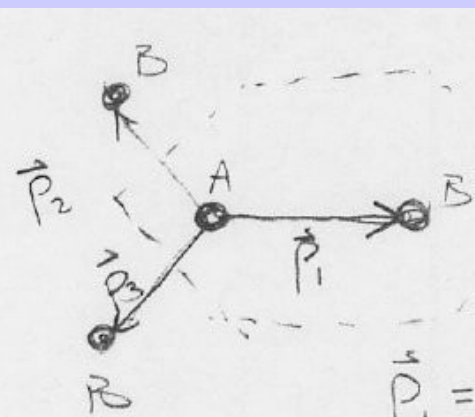
\Rightarrow Hopping is off-diagonal (from A to B)

Assume. $\psi(r) = \psi(r) e^{i\vec{k}\cdot\vec{r}}$ Bloch waves.

Then:

$$\mathcal{H} = \begin{pmatrix} 0 & t \sum_i e^{-i\vec{k}\cdot\vec{p}_i} \\ t \sum_i e^{i\vec{k}\cdot\vec{p}_i} & 0 \end{pmatrix} \quad \Rightarrow \quad E = \pm |t|^2 \left| \sum_i e^{i\vec{k}\cdot\vec{p}_i} \right|^2 = \pm |h|$$

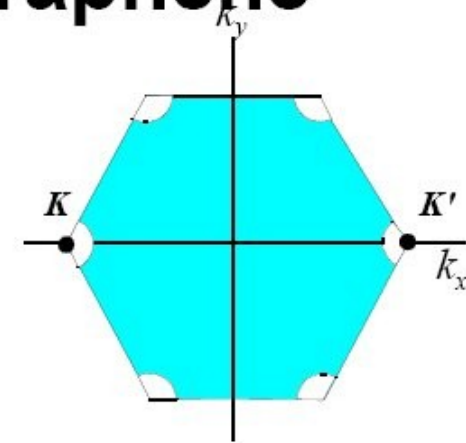
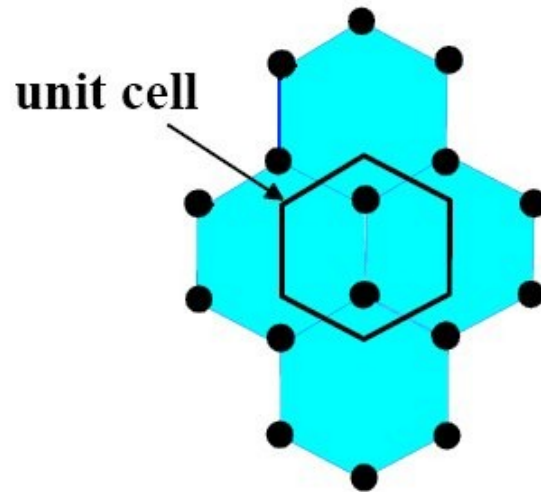
\uparrow Two roots correspond to π & π^* bands.



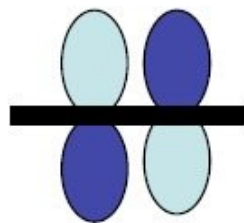
$$\vec{p}_1 = \left(\frac{1}{\sqrt{3}}, 0 \right) \\
 \vec{p}_{2,3} = \left(-\frac{1}{2\sqrt{3}}, \pm \frac{1}{2} \right)$$

Electronic Properties of Graphene

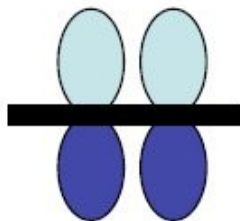
Graphene



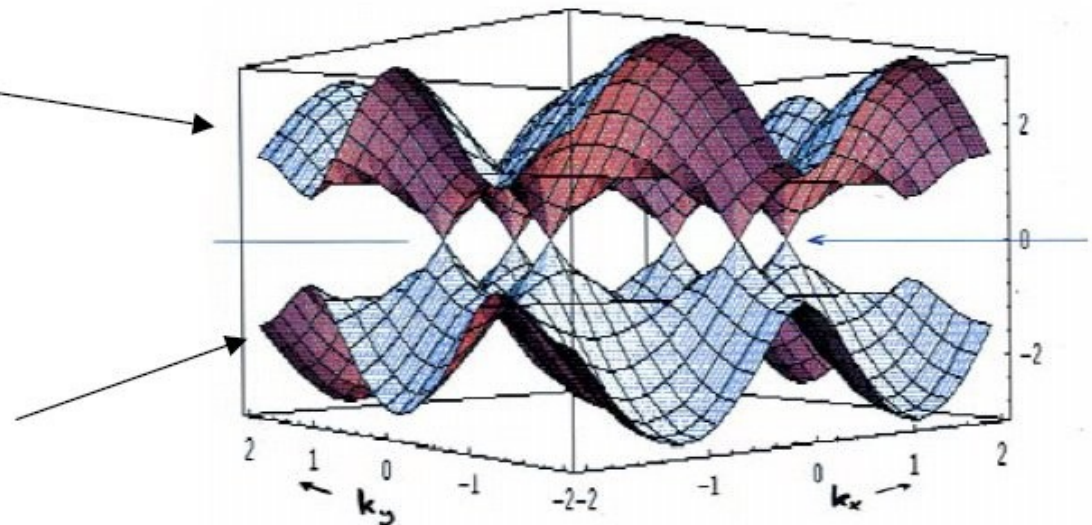
First Brillouin Zone



Anti-Bonding Orbitals



Bonding Orbitals



Linearize H near K and K'

$$h = t \left[e^{ik_x/\sqrt{3}} + e^{-\frac{ik_x}{\sqrt{3}}} 2 \cos(k_y/2) \right] \Rightarrow \text{see graph.}$$

Interesting case: $\vec{K} = \vec{K}' = (0, 4\pi/3)$.

$$h = t \left[1 + 2 \cos(2\pi/3) \right] = t \left[1 + 2(-\frac{1}{2}) \right] = 0.$$

$$E(\vec{K}) = \pm 0 \leftarrow \text{same energy}$$

\Rightarrow Gap Vanishes at $\vec{K} \leftrightarrow \vec{K}'$

What about nearby \vec{K} point?

$$\vec{k} = \vec{K} + \delta\vec{k} \Rightarrow k_x = \delta k_x \quad k_y = \frac{4\pi}{3} + \delta k_y \quad (\delta k \ll 1)$$

$$h = t \left[(1 + i\delta k_x/\sqrt{3}) + (1 - i\delta k_x/2\sqrt{3}) 2 \left[-\frac{1}{2} + (-\sin(\frac{2\pi}{3})) \delta k_y/2 \right] \right]$$

$$= t \left[\frac{\sqrt{3}}{2} i \delta k_x - \frac{\sqrt{3}}{2} \delta k_y \right]$$

$$= \frac{\sqrt{3}}{2} t (i\delta k_x - \delta k_y) \quad \text{or}$$

$$\mathcal{H} = -\frac{\sqrt{3}}{2} t \begin{pmatrix} 0 & i\delta k_x + \delta k_y \\ -i\delta k_x + \delta k_y & 0 \end{pmatrix} = A \vec{\sigma} \cdot \vec{p} \quad \begin{array}{l} \text{2D} \\ \text{Massless} \\ \text{Dirac Hamilt!} \end{array}$$

Low energy properties I

Band Structure - low energies.

Massless Dirac Fermions.

Sublattice structure \Leftrightarrow "spin"

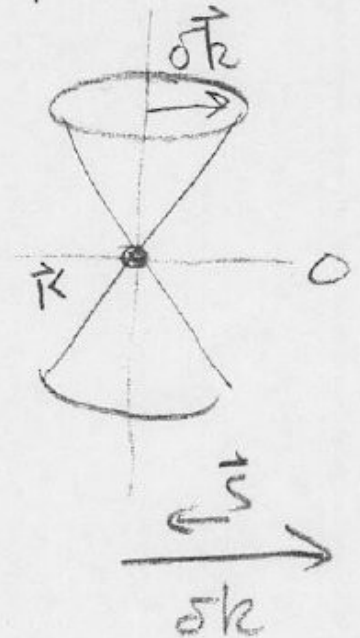
"spin" points along propagation direction (won't prove)

Putting in units, etc:

$$E_{\pm}(\delta\vec{k}) = \pm \hbar v_F (\delta k_x^2 + \delta k_y^2)^{1/2}$$

At K' , same except, "spin" is antiparallel to $\delta\vec{k}$.

\Rightarrow left & right handed fermions $\vec{s} \rightarrow \delta\vec{k}$



\Rightarrow Very Unusual 2D system!
 \Rightarrow Zero Bandgap Semiconductor.

$\frac{1}{2}(1,1) \rightarrow$ bonding $\rightarrow +s_x$
 $\frac{1}{2}(1,-1) \rightarrow$ antibonding $\rightarrow -s_x \dots$

Low energy properties II

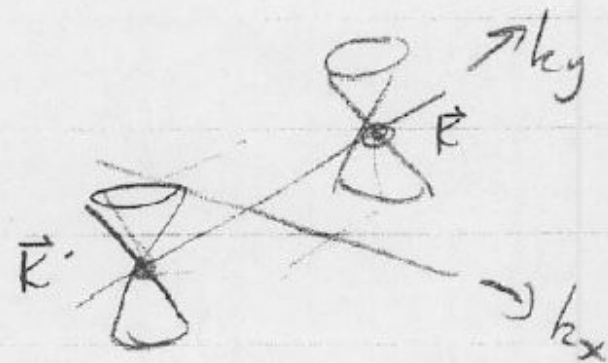
Unlike "massive" 2D system \Rightarrow DOS not constant.

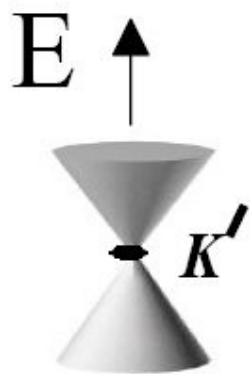
LL's not equally spaced, etc.

New experiments (Gem et al, Kim et al) on single sheets underway!

Summary \Rightarrow Band structure set
by 2 2D Dirac cones

$$v_F = 8 \cdot 10^5 \text{ m/s}$$





left-handed

Low energy theory: 2D massless Dirac Fermions

Dirac ($k \cdot p$) Hamiltonian

$$H = \hbar v_F \boldsymbol{\sigma} \cdot \mathbf{k}$$

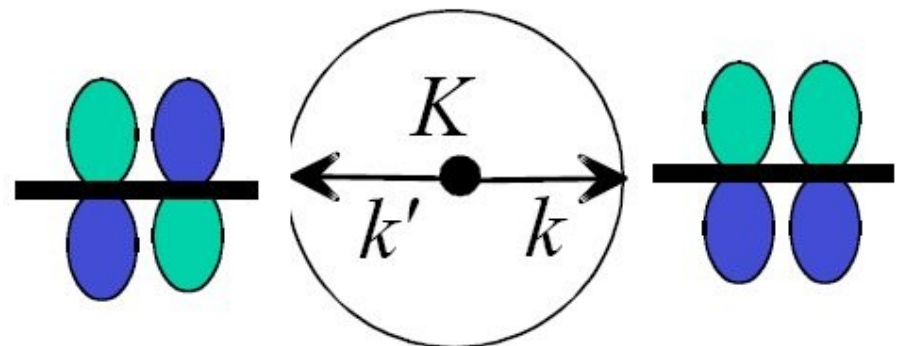
$$E = \hbar v_F |k|$$

$$|k\rangle = \frac{1}{\sqrt{2}} e^{ik\phi} \begin{pmatrix} -i b e^{-i\theta_k/2} \\ e^{i\theta_k/2} \end{pmatrix}$$



right-handed

“spin” = molec. orbital state



Relativistic electron in magnetic field

$$E_n = \text{sgn}(n) |n|^{1/2} \epsilon_0, \quad \epsilon_0 = \hbar v_0 (2eB / \hbar c)^{1/2}$$

Particle-hole symmetric; has a *zero mode*

$$E_n \propto \sqrt{n}, \sqrt{B}$$

Separation between low-lying LL is very large,
1000 K at $B = 10$ T \longrightarrow *room temperature QHE*

Explanation: $H_{\text{Pauli-Schroedinger}} = 2m(H_{\text{Dirac}})^2$

Square root dependence tested by infrared spectroscopy

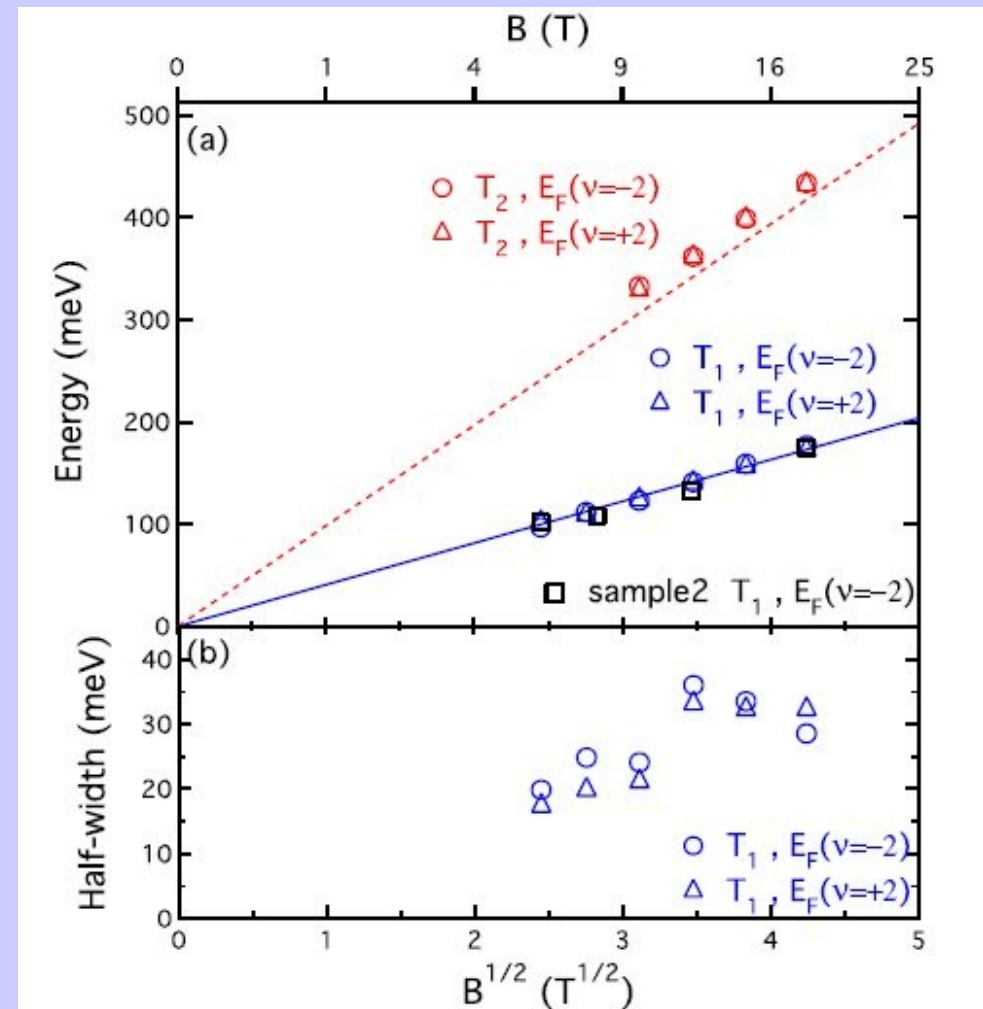
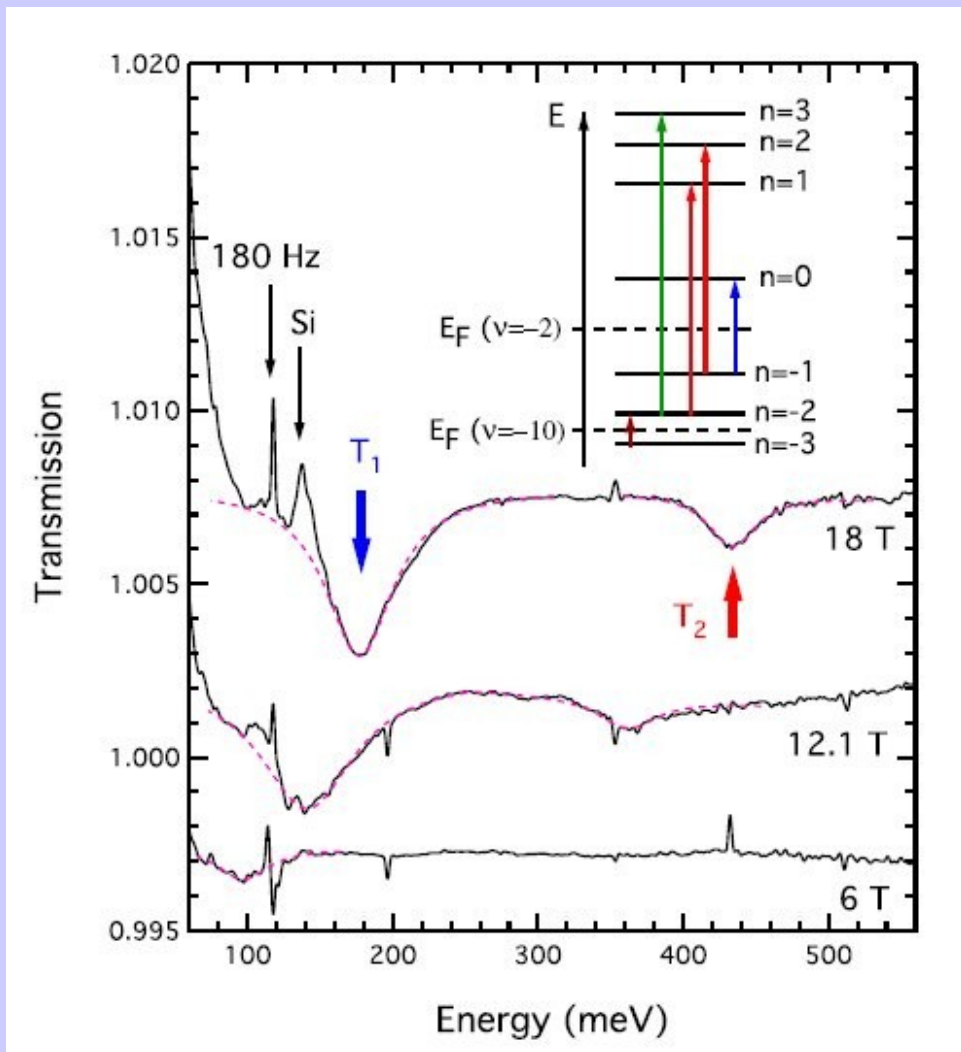


FIG. 3 (color online). (a) Resonance energies vs \sqrt{B} , from holes (ratio of $\nu = -2$ and $\nu = -10$ data, Fig. 2) and electrons

Stormer, Kim (Columbia University)

Lecture I
Dirac electrons
in external fields:

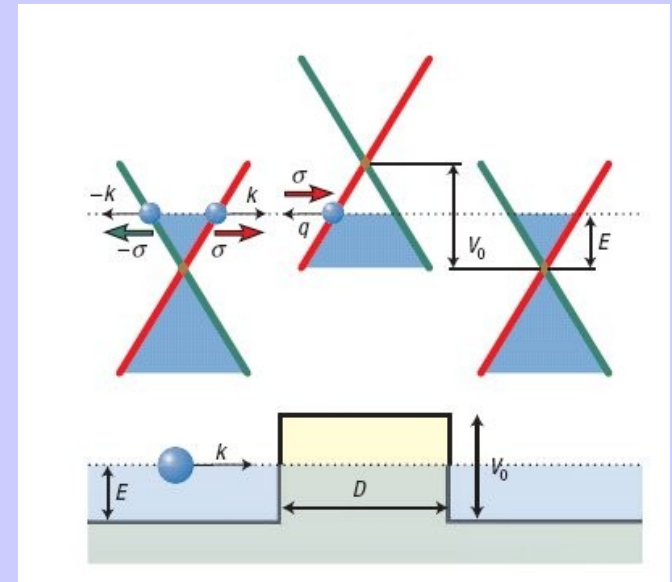
chiral dynamics,
Klein paradox,
transport in p-n junctions

Klein tunneling

Klein paradox: transmission of relativistic particles is unimpeded even by highest barriers
 Reason: negative energy states;
 Physical picture: particle/hole pairs

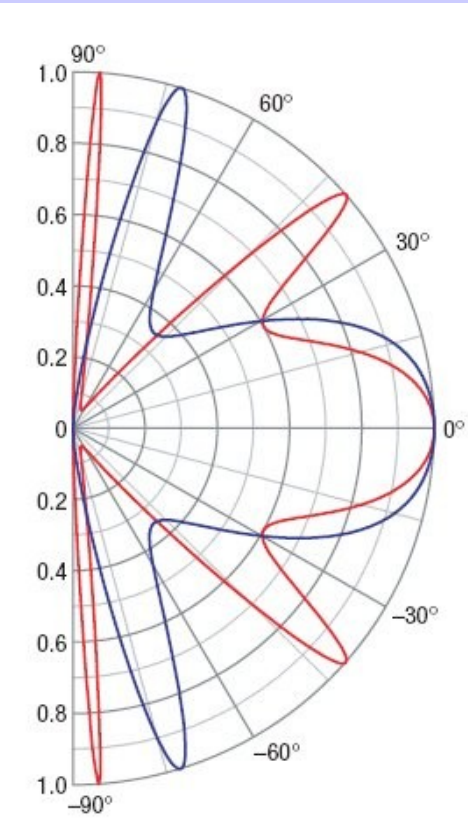
Katsnelson, Novoselov, Geim

Example: potential step



$$V(x) = \begin{cases} V_0, & 0 < x < D, \\ 0 & \text{otherwise.} \end{cases}$$

Transmission angular dependence



Chiral dynamics of massless Dirac particles: no backward scattering (perfect transmission at zero angle)

$$\psi_1(x, y) = \begin{cases} (e^{ik_x x} + r e^{-ik_x x}) e^{iky}, & x < 0, \\ (a e^{iq_x x} + b e^{-iq_x x}) e^{iky}, & 0 < x < D, \\ t e^{ik_x x + iky}, & x > D, \end{cases}$$

$$\psi_2(x, y) = \begin{cases} s(e^{ik_x x + i\phi} - r e^{-ik_x x - i\phi}) e^{iky}, & x < 0, \\ s'(a e^{iq_x x + i\theta} - b e^{-iq_x x - i\theta}) e^{iky}, & 0 < x < D, \\ s t e^{ik_x x + iky + i\phi}, & x > D, \end{cases}$$

Limit of extremely high barrier: finite T

$$T = \frac{\cos^2 \phi}{1 - \cos^2(q_x D) \sin^2 \phi}$$

Confinement problem

No discrete spectrum, instead:
quasistationary states (resonances)

Silvestrov, Efetov

Classical trajectories

Example: parabolic potential
 $V(x) = U(x/x_0)^2 + E$

$$H_{\text{eff}} = \varepsilon = \pm c\sqrt{p_x^2 + p_y^2} + V(x).$$

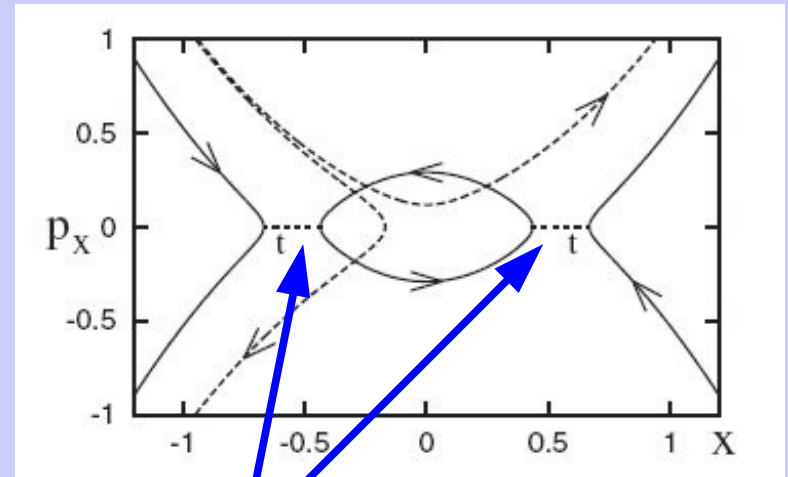
Bohr-Sommerfeld quantization

$$\int_{x_{\text{in}-}}^{x_{\text{in}+}} \sqrt{[\varepsilon_N - V(x)]^2 - c^2 p_y^2} \frac{dx}{c} = \pi\hbar \left(N + \frac{1}{2} \right).$$

Finite lifetime

$$\Gamma_N = \frac{\hbar}{\Delta t} w = \frac{\hbar v_0}{2x_0} \sqrt{\frac{U}{-2\varepsilon_N}} \exp\left(-\frac{\pi c p_y^2 x_0}{\hbar \sqrt{-2\varepsilon_N U}}\right).$$

Relation
to exp?

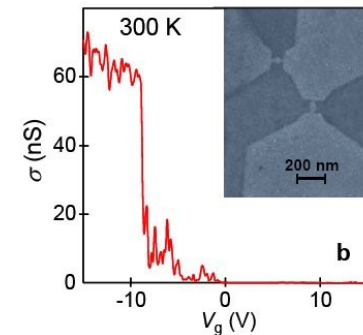
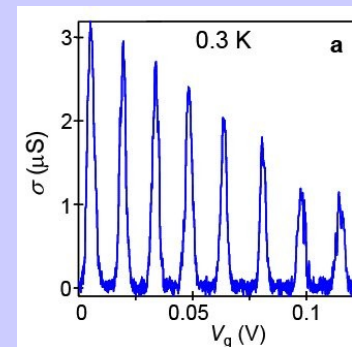


Tunneling

Turning points:

$$\frac{x_{\text{out}\pm}}{x_0} = \pm \sqrt{2 \frac{c|p_y| - \varepsilon}{U}},$$

$$\frac{x_{\text{in}\pm}}{x_0} = \pm \sqrt{2 \frac{-c|p_y| - \varepsilon}{U}}.$$



Electron in a p-n junction

Potential step instead of a barrier (smooth or sharp)

Cheianov, Falko 2006

p-n junction schematic:

$$H = e\varphi(\mathbf{x}) + v_F \xi \begin{pmatrix} 0 & p_+ \\ p_- & 0 \end{pmatrix}, \quad p_{\pm} = p_1 \pm ip_2.$$

+1(-1) for points K(K')

smooth step:

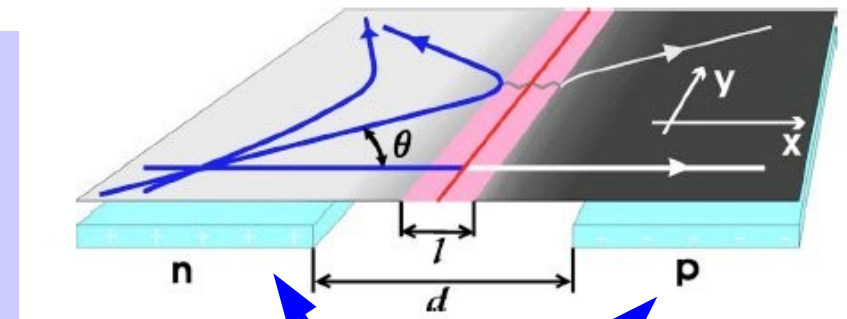
sharp step:

$$w(\theta) = e^{-\pi(k_F d)\sin^2 \theta}.$$

$$w_{\text{step}}(\theta) = \cos^2 \theta$$

(nontrivial)

(straightforward)



gates

In both cases, perfect transmission in the forward direction: manifestation of chiral dynamics

p-n junction in magnetic field

Relativistic motion in crossed E, B fields: Lorentz invariants $E^2 - B^2$, $E \cdot B$
 electric case $E > B$ (“parabolic trajectories”)
 and magnetic case $B > E$ (cyclotron motion with drift)

Shytov, Nan Gu, LL

Dirac equation (4) in a Lorentz-invariant form

$$\gamma^\mu (p_\mu - a_\mu) \psi = 0, \quad \{\gamma_\mu, \gamma_\nu\}_+ = 2g_{\mu\nu}, \quad (7)$$

where γ^μ are Dirac gamma-matrices, $\gamma^0 = \sigma_3$, $\gamma^1 = -i\sigma_2$, $\gamma^2 = -i\sigma_1$, and ψ is a two-component wave function.

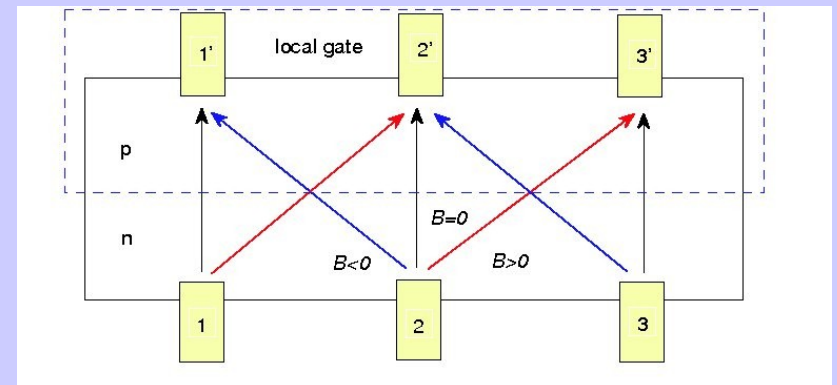
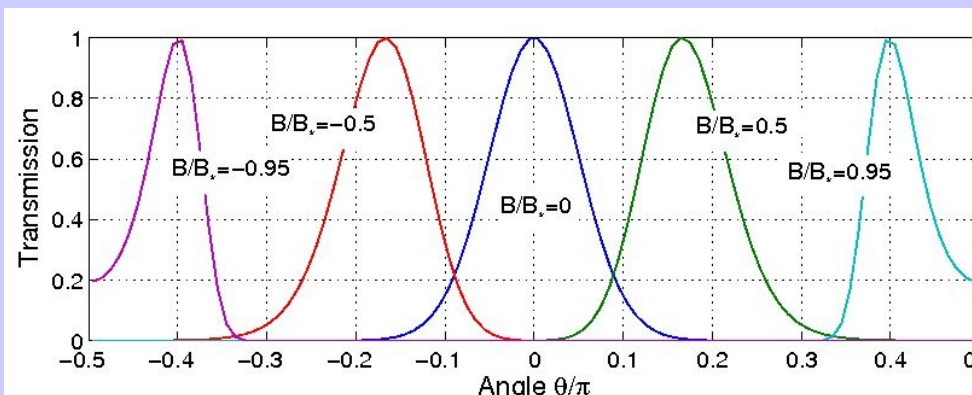
$$a_0 = -\frac{e}{v_F} E y, \quad a_1 = -\frac{e}{c} B y, \quad a_2 = 0.$$

Critical field $B = B_* \equiv (c/v_F)E$.

Electric regime $B < (c/v_F)E$, Magnetic regime (QHE, $G=0$) $B > (c/v_F)E$

Perfect, collimated transmission at a finite angle $\theta_B = \arcsin B/B_*$
 net conductance suppressed

electric case



No magnetic field: $E > 0$, $B = 0$

Quasiclassical WKB analysis

Evolution with a non-hermitian Hamiltonian

$$i\partial_x \psi(x) = ((\varepsilon + ax)\sigma_2 + i(p_1 + bx)\sigma_3) \psi(x).$$

Eigenvalues:

$$\kappa(x) = \sqrt{(\varepsilon + ax)^2 - (p_1 + bx)^2}$$

$$S = 2 \int_{x_1}^{x_2} \text{Im} \kappa(x) dx = \pi \frac{(p_1 a - \varepsilon b)^2}{(a^2 - b^2)^{3/2}}$$

$$T(p_1) = \exp(-\pi \hbar v_F p_1^2 / |eE|),$$

Exact solution: use momentum representation (direct access to asymptotic plane wave scattering states)

$$-ieE d\psi/dp_2 = \tilde{H} \psi, \quad \tilde{H} = v_F(p_1 \sigma_1 - p_2 \sigma_2) - \varepsilon.$$

Equivalent to Landau-Zener transition

Interpretation: interband tunneling for $p_2(t) = vt$

LZ result matches WKB

Finite B-field:

Eliminate B with
the help of a Lorentz boost:

Aronov, Pikus 1967

$$\Lambda = \begin{pmatrix} \gamma & \gamma\beta & 0 \\ \gamma\beta & \gamma & 0 \\ 0 & 0 & 1 \end{pmatrix}, \quad \gamma = \frac{1}{\sqrt{1-\beta^2}}$$

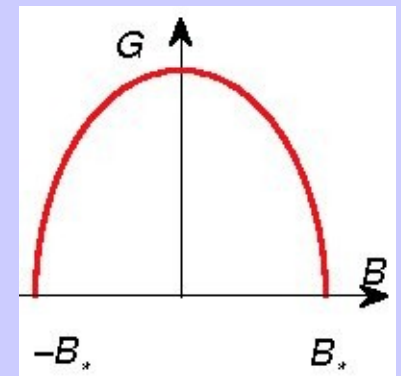
Transmission coefficient is Lorentz-invariant:

$$T(p_1) = e^{-\pi\gamma^3 d^2 (p_1 + \beta\varepsilon)^2}, \quad d = (\hbar v_F / |eE|)^{1/2}$$

Net conductance (Landauer formula):

$$G = \frac{e^2}{h} \sum_{-k_F < p_1 < k_F} T(p_1) = \frac{we^2}{2\pi h} \int_{-k_F}^{k_F} T(p_1) dp_1$$

$$G(B \leq B_*) = \frac{e^2}{2\pi h} \frac{w}{d} (1 - (B/B_*)^2)^{3/4}$$



Suppression of conductance in the electric regime precedes
formation of Landau levels and edge states in p-n junction
In the magnetic regime: no bulk transport, only edge transport

Transport in E and B fields, Manifestations of relativistic Dirac physics:

- ◆ Klein tunneling via Dirac sea of states with opposite polarity;
- ◆ chiral dynamics (perfect transmission at normal incidence);
- ◆ electric and magnetic regimes $B < 300E$ and $B > 300E$ ($300 = c/v_F$)
- ◆ Consistent with negligibly low intrinsic resistance of existing p-n junctions

HW?

Lecture II

Graphene Quantum Hall effect

QHE basics;
half-integer QHE;
edge states in graphene;
QHE in p-n junctions;
spin transport

Background on QHE

General 2D physics

Parabolic spectrum $E(p)=p^2/2m$

Bob Willett's
lecture notes

No B-field

$n =$ electron density, N/l^2

$$2N (\lambda/2)^2 = \pi l^2$$

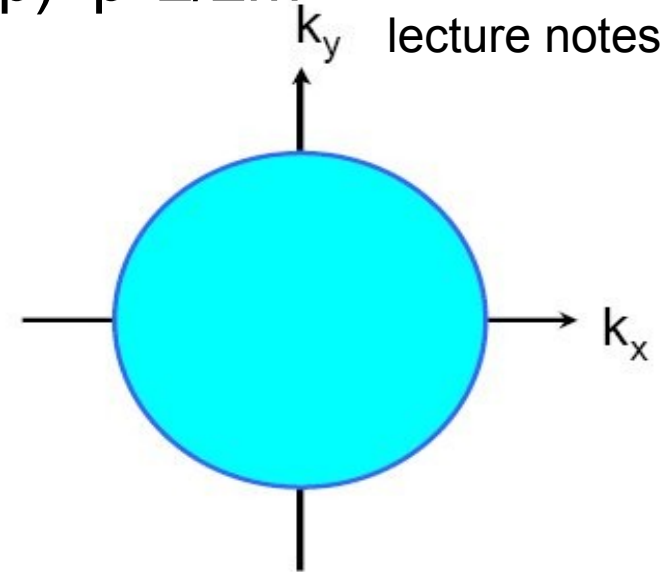
$$k = 2\pi/\lambda$$

filled Fermi sea up to

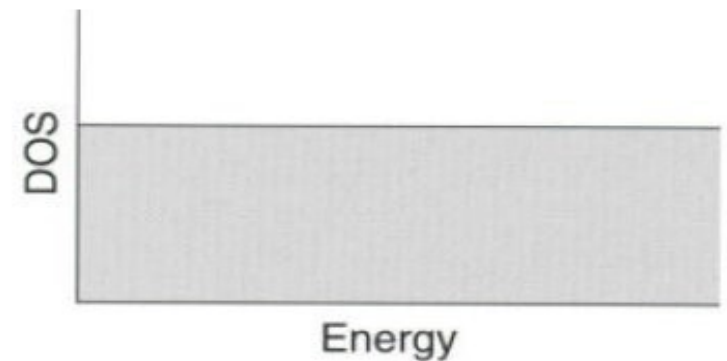
$$k_F = (2\pi n)^{1/2}$$

$$\text{DOS} = dn/dE, \quad n = m E_F / \pi \hbar^2$$

$$dn/dE = m / \pi \hbar^2 = \text{constant}$$



$$k_F = (2\pi n)^{1/2}$$



Quantum Hall effect

General 2D physics

With B-field

Hamiltonian

$$H = \frac{(\vec{p} + e\vec{A})^2}{2m^*} + \frac{1}{2} g\mu_B \vec{\sigma} \cdot \vec{B} + V(z)$$

energy eigenvalues

$$E_n = (N + \frac{1}{2}) \hbar\omega_c + \frac{1}{2} g\mu_B B + E_0$$

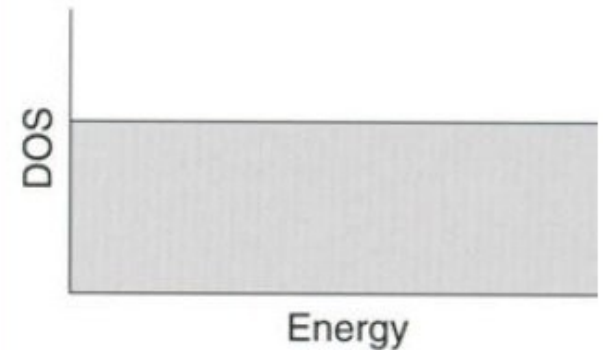
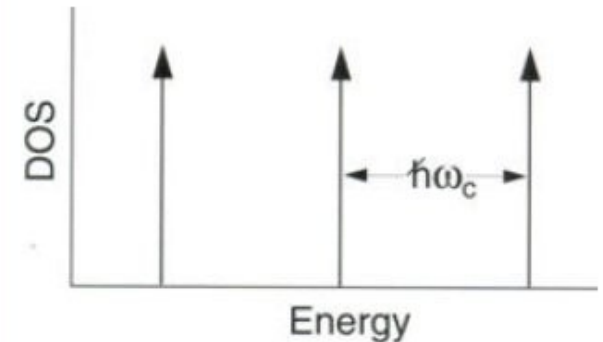
$$m^*/m_0 = 0.067, \quad g = -0.44$$

$$\text{cyclotron frequency } \omega_c = eB/m^*$$

$$\text{density of states } D = eB/h$$

$$\text{Bohr magneton } \mu_B = e\hbar/2m_0$$

$$\hbar\omega_c = 20 \text{ K at } B = 1 \text{ T}; \quad g\mu_B B \sim \hbar\omega_c / 70$$



Quantum Hall effect

General 2D physics

With B-field (cont.)

$$H = \frac{(\vec{p} + e\vec{A})^2}{2m^*}$$

symmetric gauge: $\vec{A} = \frac{1}{2}(\vec{r} \times \vec{B})$

$$\psi_{0,N} = z^j e^{-|z|^2/4} u^{(j)}, \quad j = 0, 1, 2, \dots$$

$N=0 \nearrow$
 $z = (x + iy)$

Landau gauge: $\vec{A} = -yB\hat{x}$

$$\psi_{N,k} = e^{ikx} v_N(y - y_k)$$

Guiding center of cycl. orb.

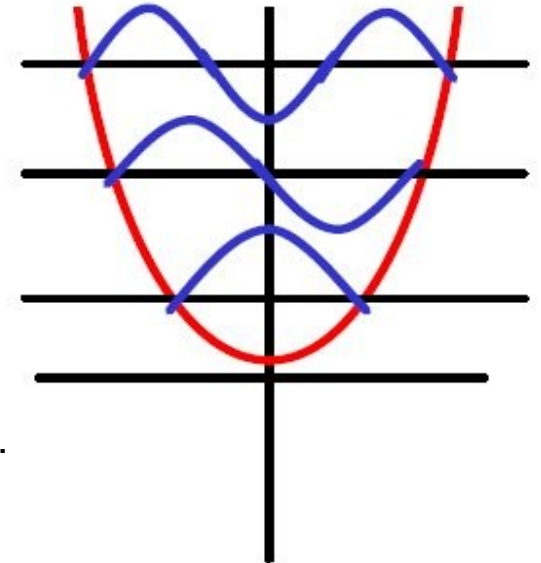
$$v_N(\alpha) = e^{-\alpha^2/2l^2} H_N(\alpha)$$

$$y_k = kl^2$$

$$l^2 = \hbar/eB, \text{ magnetic length}$$

note nodal structure for $N > 0$

Higher Landau levels have more nodes



Magnetic length l_0

Momentum-position duality

Quantum Hall effect

General 2D physics

With B-field and disorder

scattering times

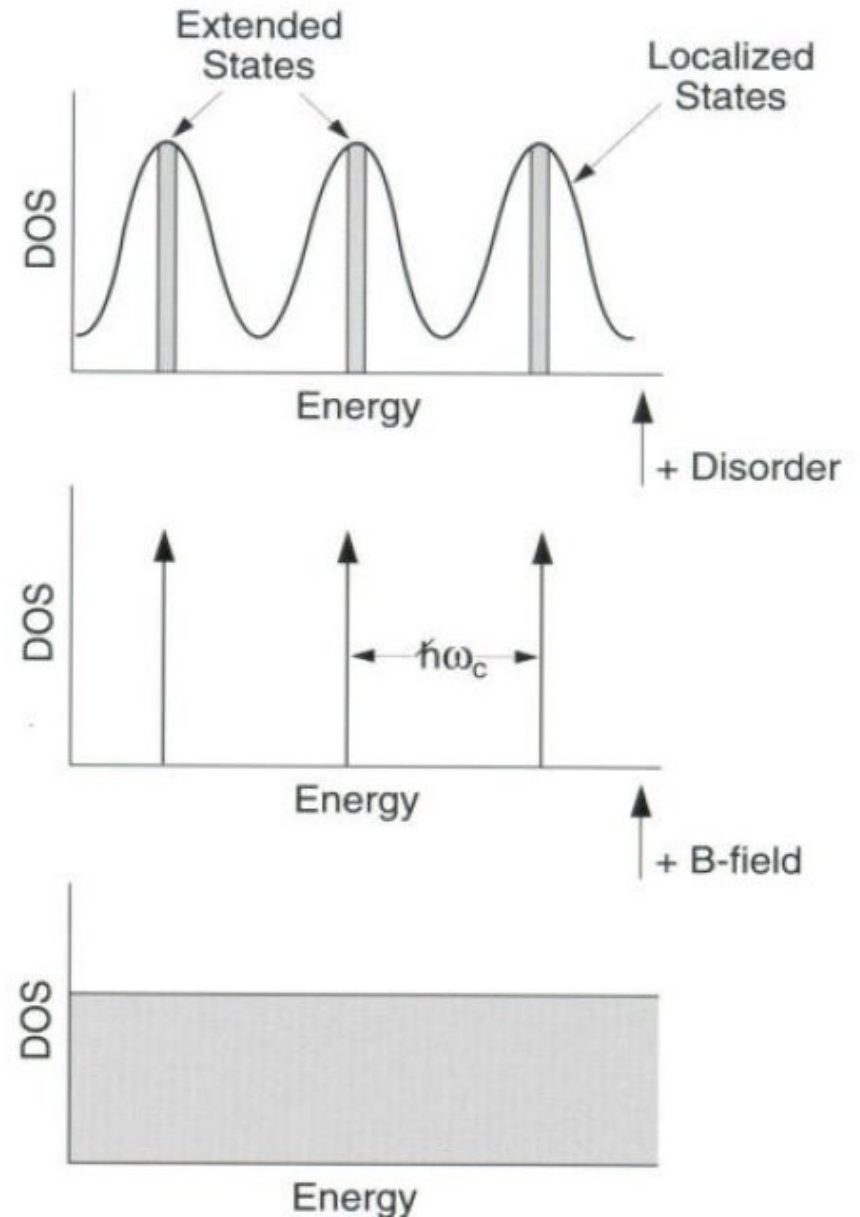
a) level broadening $\Gamma = \hbar/\tau$
relaxation time $\tau \equiv$
time to be scattered into a
different state

$\omega_c \tau \gg 1 \Rightarrow$ resolved
Landau levels

b) transport scattering time
mean-free-path $l_{mp} = v_F \tau_{tr}$

mobility $\mu \equiv v/E$; $\mu = \frac{1}{ne\rho}$
 $\rho =$ resistivity, $n =$ areal density

$$\sigma = ne\mu = ne^2 \tau_{tr} / m$$



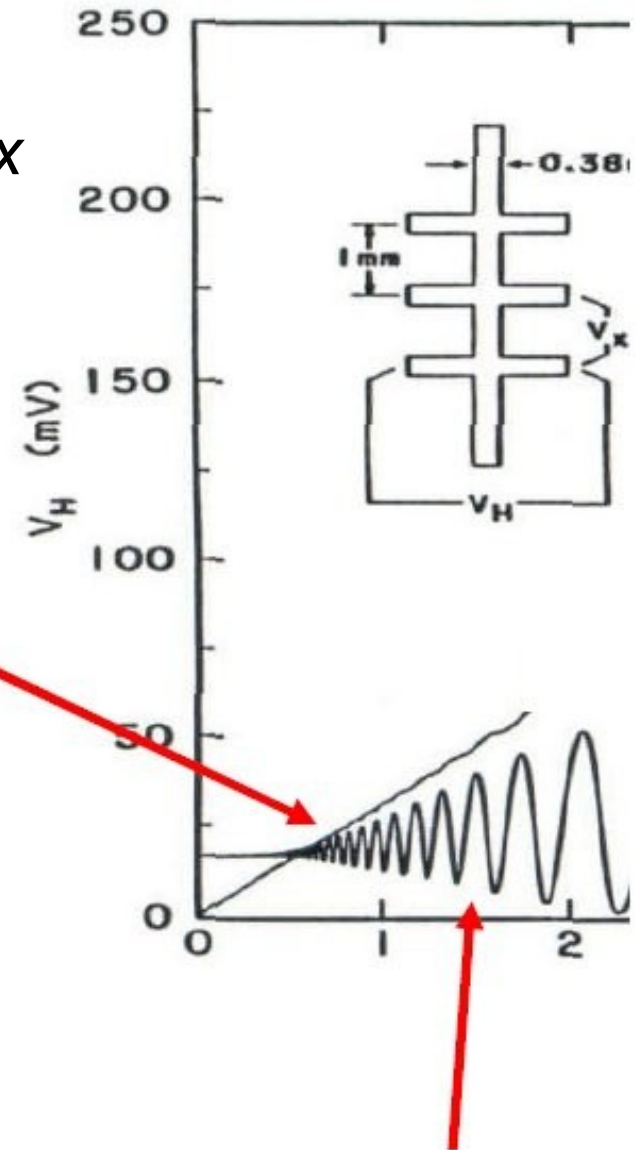
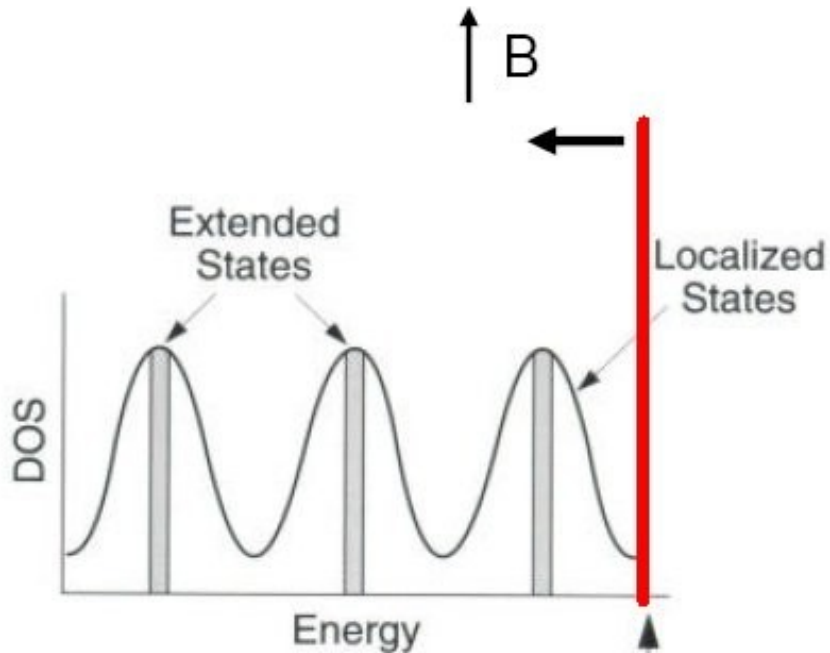
QHE measurement I

Measurements – Hall effect

*Measured quantities are R_{xx} , R_{xy} ,
find σ_{xx} , σ_{xy} by inverting a 2x2 matrix*

With increasing B, degeneracy of LL increases and Fermi level is swept through spectrum (constant density n)

Landau levels resolved

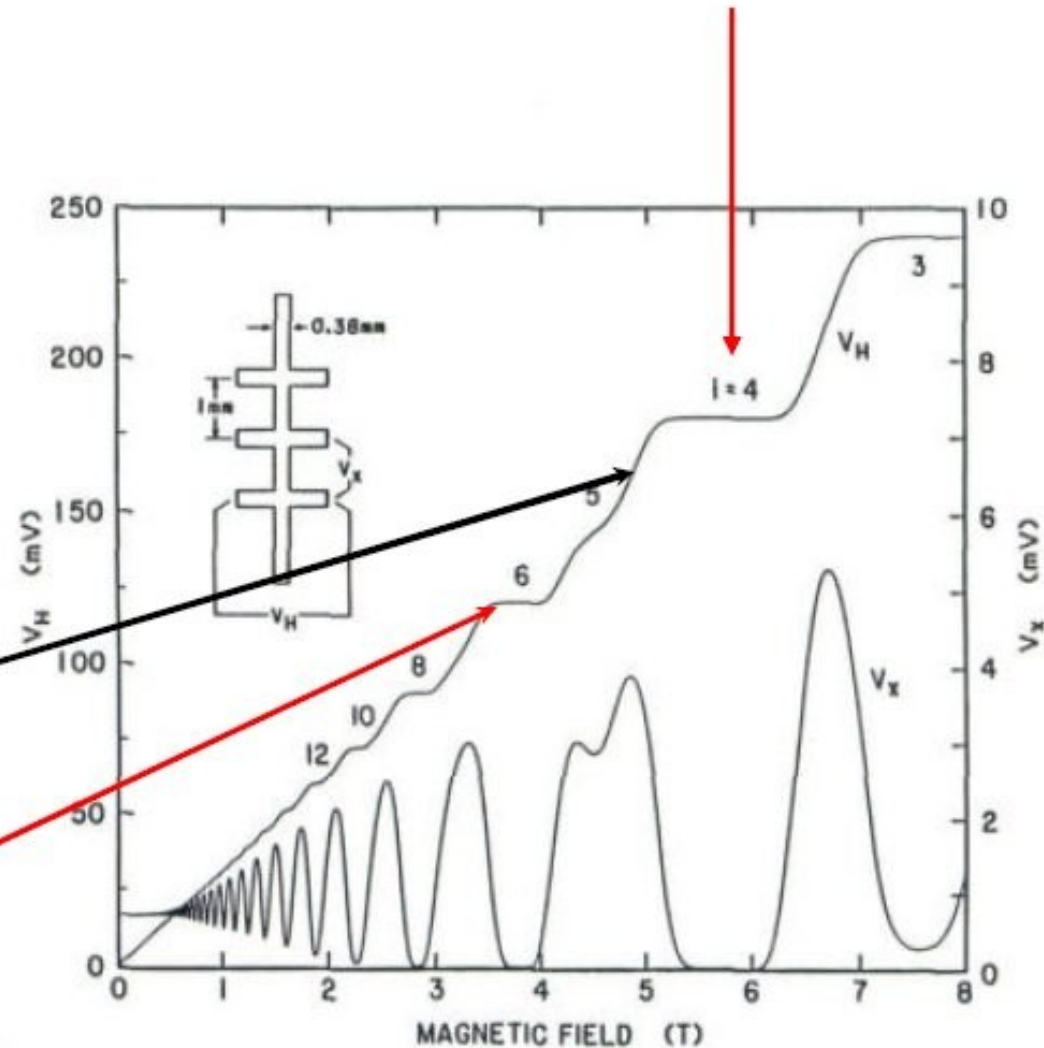
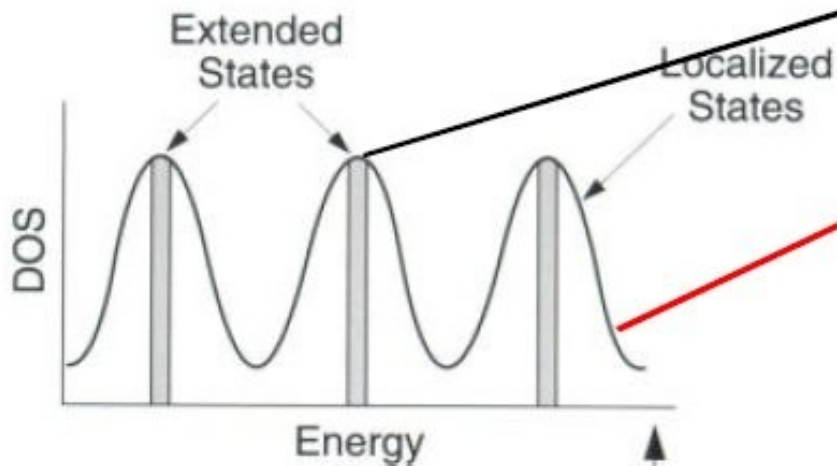


Shubnikov-deHaas oscillations

QHE measurement II

Measurements – quantum Hall effect

At extended states, the Hall voltage increases



Localization of single electrons between extended states produces plateaus in Hall resistance

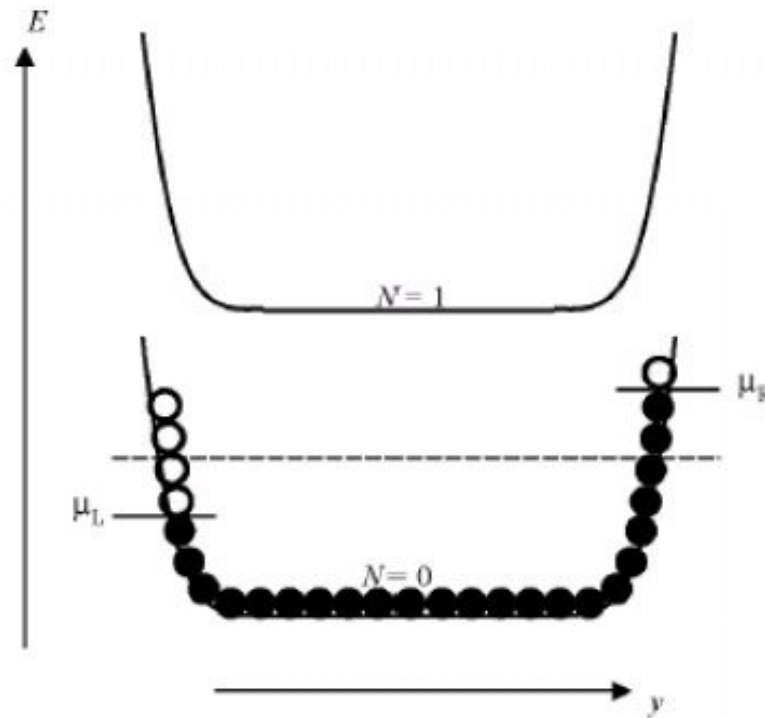
QHE: edge transport

Measurements – quantum Hall effect

Integer QHE and Edge States

Chiral dynamics
along edge
(unidirectional)

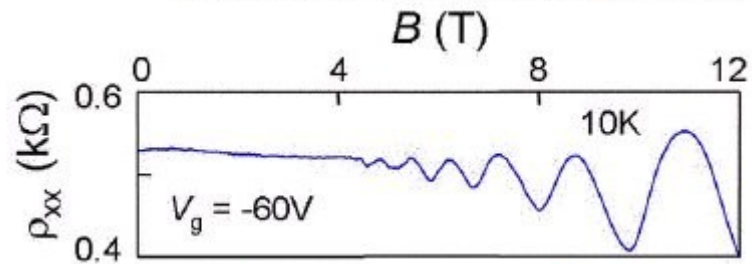
Edge conduction



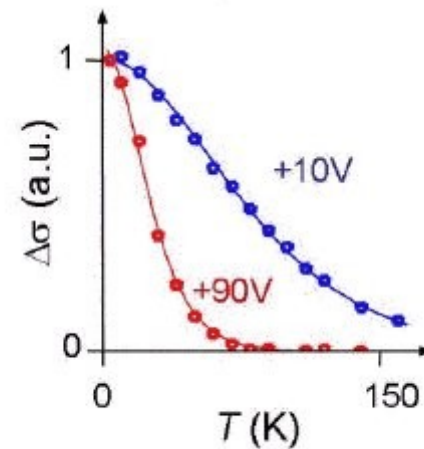
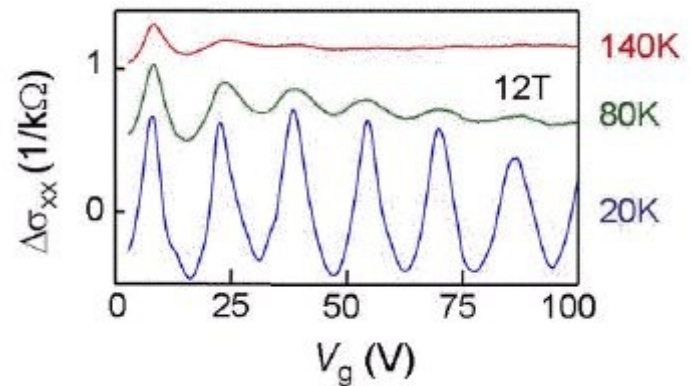
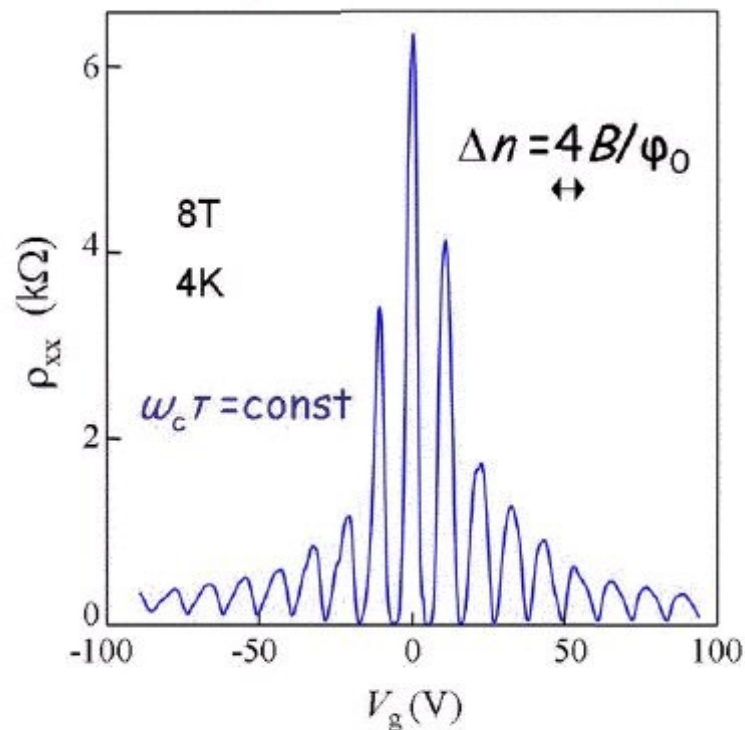
No
backscattering
along same
edge

$$I = \sum_{occ.} i_k = \int \frac{L_x dy_k}{2\pi \ell^2} \left(\frac{\partial \varepsilon_N}{\partial y_k} \frac{e \ell^2}{\hbar L_x} \right) = \frac{e}{h} (\mu_R - \mu_L) = \frac{e^2}{h} V_H$$

Quantum Oscillations in Graphene



degeneracy $f=4$
two spins & two valleys



$$\Delta\sigma_{xx} \propto T / \sinh\left(\frac{2\pi^2 k_B T m_c}{\hbar e B}\right)$$

The "half-integer" QHE in graphene

Single-layer graphene:
QHE plateaus observed at

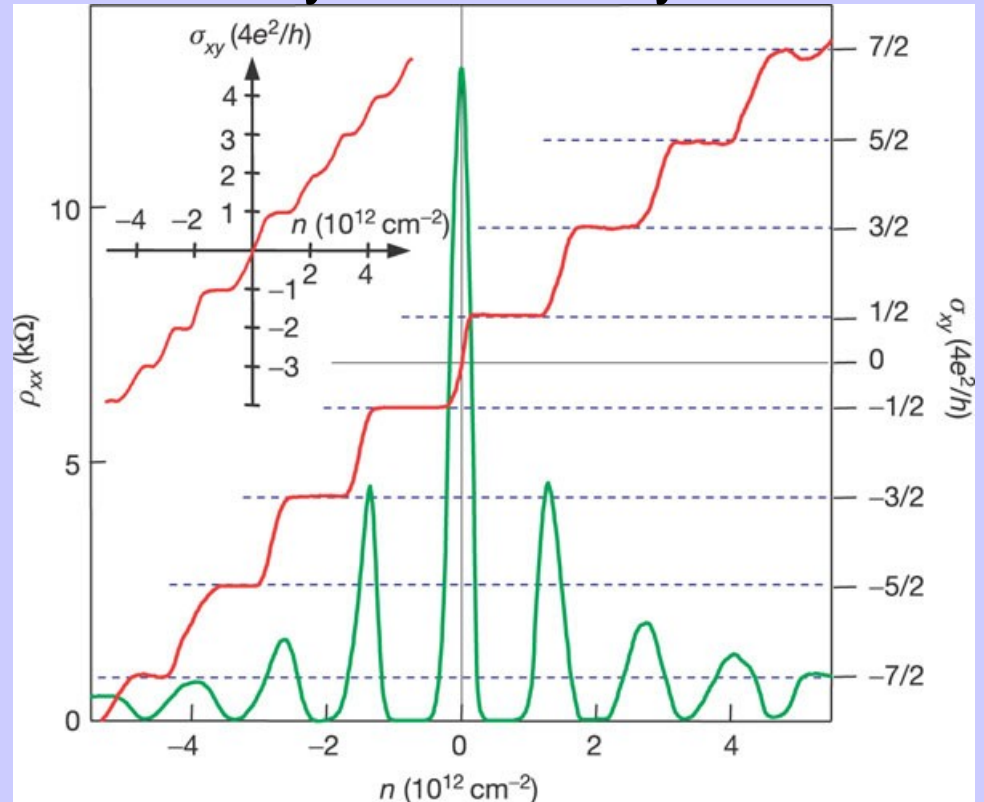
$$\nu = 4 \times (0, \pm 1/2, \pm 3/2 \dots)$$

4=2x2 spin and valley degeneracy

Explanations of half-integer QHE:

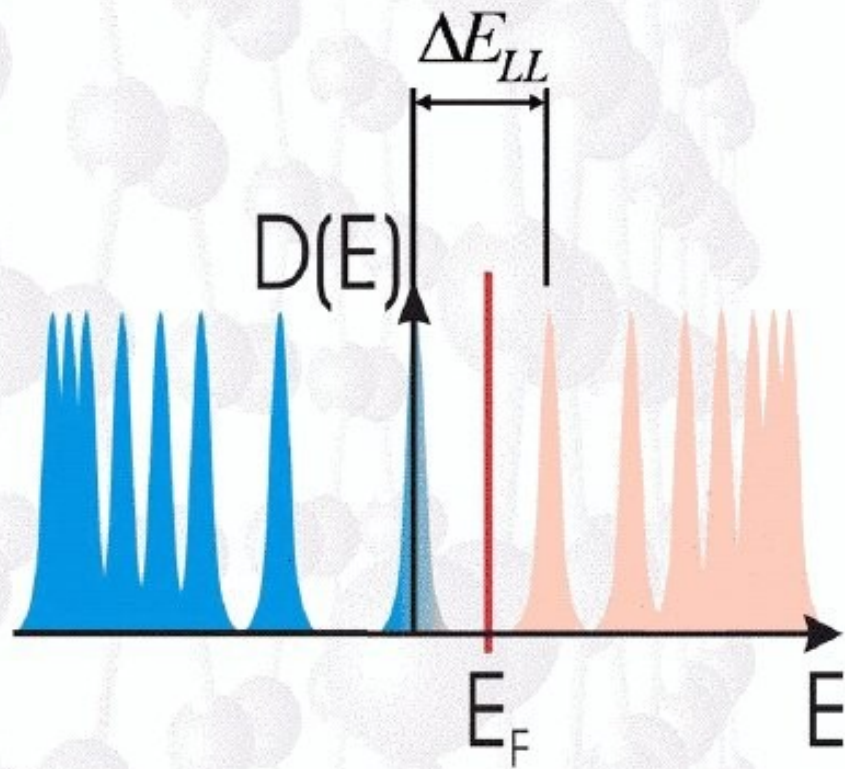
- (i) anomaly of Dirac fermions;
- (ii) Berry phase;
- (iii) counter-propagating edge states

double-layer: one layer:



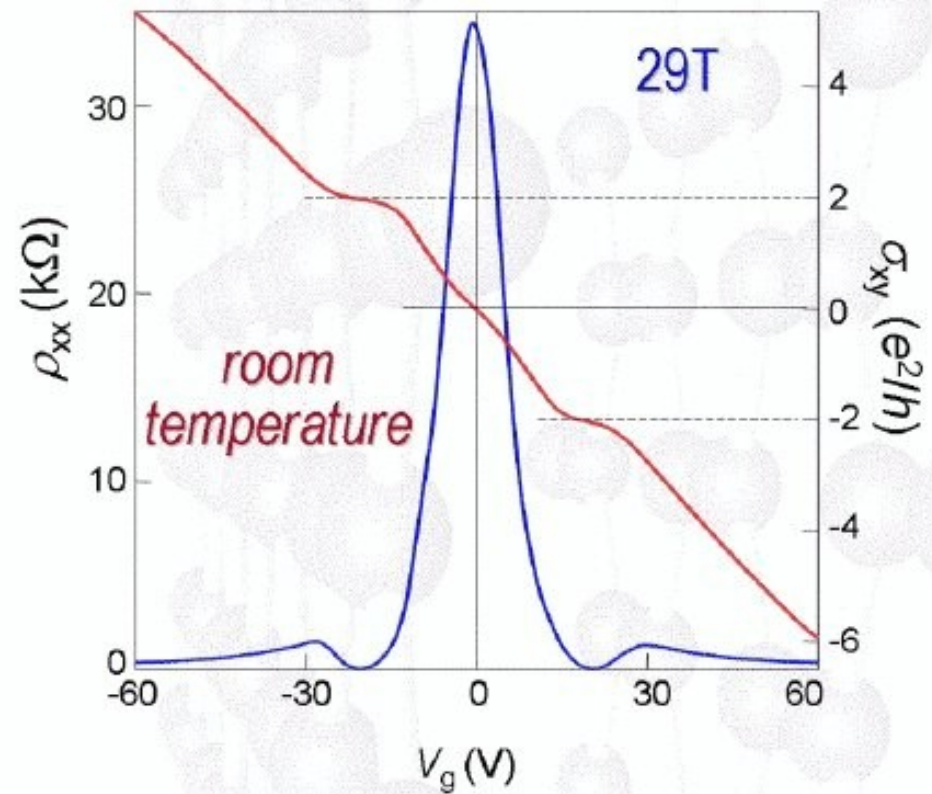
Novoselov et al, 2005, Zhang et al, 2005

room-temperature QHE



$$\Delta E_{LL} = v_F \sqrt{2e\hbar B}$$

$$\Delta E_{LL} (K) = 420 \sqrt{B(T)}$$



*previously,
only below 30K*

The half-integer quantization from Berry's phase

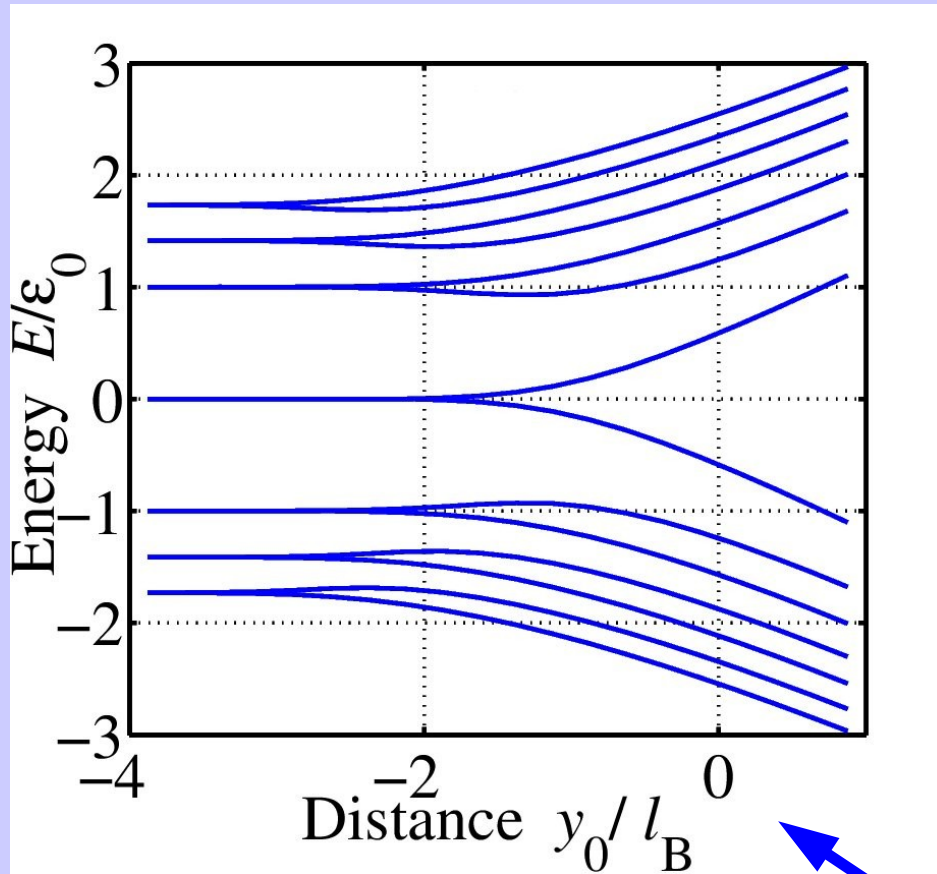
Quasiclassical Landau levels (nonrelativistic):
Bohr-Sommerfeld quantization for electron energy
in terms of integer flux $\Phi = n\Phi_0$ enclosed by a cyclotron orbit

For chiral massless relativistic particles (pseudo)spin is parallel
to velocity, subtends solid angle 2π upon going over the orbit:
quantization condition modified as $\Phi = (n + 1/2)\Phi_0$

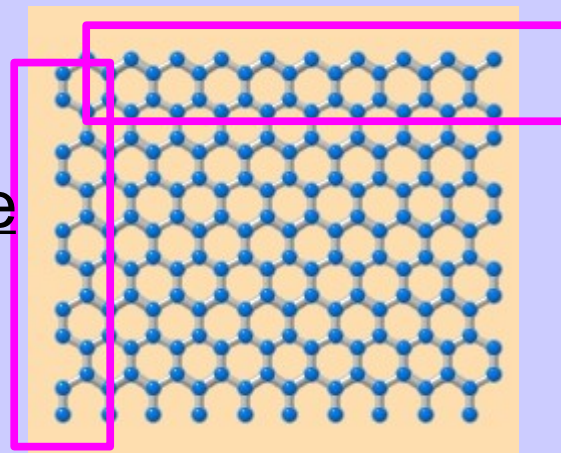
Prediction of half-period shift of Shubnikov-deHaas oscillation

Translates into half-integer QHE in quantizing fields

Edge states for graphene QHE



armchair edge



zigzag edge
(similar, +surface states)

Edge states properties:

- KK' splitting due to mixing at the boundary;
- Counter-propagating electron and hole states;
- Symmetric splitting of $n=0$ LL
- Universality, same for other edge types;
- The odd numbers of edge modes result in half-integer QHE

Edge states from 2d Dirac model

Abanin, Lee, LL, PRL 96, 176803 (2006)

Also: Peres, Guinea, Castro-Neto, 2005, Brey and Fertig, 2006

The half-integer QHE: Field-Theoretic Parity Anomaly

R. Jackiw, Phys.Rev D29, 2377 (1984)

A novel axial anomaly has been found in gauge theories defined on three-dimensional space-time, which describe dynamics confined to a plane: fermions moving in an external gauge field and governed by the 2×2 matrix equation (massless Dirac equation)

$$\gamma^\mu (i\partial_\mu - eA_\mu) \Psi = 0 \quad (1)$$

induce a topologically nontrivial vacuum current of abnormal parity,

$$\langle j^\mu \rangle = \pm c \frac{e}{8\pi} \epsilon^{\mu\alpha\beta} F_{\alpha\beta} + \dots \quad (2)$$

Recognize Lorentz-invariant QHE relation
 $j = \sigma_{xy} E$, where $\sigma_{xy} = 1/2$

Here γ^μ are three 2×2 "Dirac" matrices (Pauli matrices) and A_μ is the external vector potential, leading to the field strength $F_{\alpha\beta}$.

Anomaly: relation to fractional quantum numbers

The purpose of this paper is to derive similar results in the three-dimensional case under present discussion. We show that for static background fields in the $A_0=0$ Weyl gauge, the Dirac Hamiltonian corresponding to (1) possesses a conjugation-symmetric spectrum with zero modes, if the background field satisfies certain requirements. Although the topological interest is mainly in the non-Abelian theory, we shall concern ourselves with the Abelian Maxwell theory, which is of greater physical relevance, since it can describe the motion of charged fermions on a plane perpendicular to an external magnetic B field.

The demonstration is very simple. The Hamiltonian corresponding to (1) is

$$H = \vec{\alpha} \cdot (\vec{p} - e\vec{A}) , \quad (3)$$

where the “Dirac” $\vec{\alpha}$ matrices are the two Pauli matrices: $\alpha^1 = -\sigma^2$, $\alpha^2 = \sigma^1$. The β matrix, which would be present if there were a mass term, is taken to be σ^3 . Since $\beta = \sigma^3$ anticommutes with H , it serves as a conjugation matrix, and the energy eigenmodes are symmetric about $E=0$,

$$\vec{\alpha} \cdot (\vec{p} - e\vec{A})\psi_E = E\psi_E , \quad (4)$$

$$\sigma^3\psi_E = \psi_{-E} .$$

Of course in the presence of the mass term, the conjugation symmetry is broken.

To find the zero-energy modes we write the wave function as $\psi_0 = \begin{pmatrix} u \\ v \end{pmatrix}$, and choose the Coulomb gauge for \vec{A} , which we assume to be single valued and well behaved at the origin,

$$A^i = \epsilon^{ij} \partial_j a , \quad (5)$$

$$B = -\nabla^2 a . \quad (6)$$

Then Eq. (4) reduces to the pair

$$(\partial_x + i\partial_y)u - e(\partial_x + i\partial_y)au = 0 , \quad (7)$$

$$(\partial_x - i\partial_y)v + e(\partial_x - i\partial_y)av = 0 ,$$

with the obvious solution

$$u = \exp(ea)f(x+iy) , \quad (8)$$

$$v = \exp(-ea)g(x-iy) ,$$

where f and g are arbitrary entire functions. Thus we can form self-conjugate solutions $\begin{pmatrix} u \\ 0 \end{pmatrix}$ and $\begin{pmatrix} 0 \\ v \end{pmatrix}$. Whether these are acceptable wave functions depends on the large- r behavior of a . If a grows sufficiently rapidly at large distance, then either u or v will be normalizable, and there exist one or more isolated zero-energy bound states, the multiplicity depending on how many different forms for f or g may be taken.

It is useful to classify the various possibilities in terms of the total flux, which is also proportional to the total induced charge:

$$\langle j^0 \rangle = \pm \frac{e}{4\pi} B , \quad (9)$$

$$Q = \int d^2\vec{r} \langle j^0 \rangle = \pm \frac{e}{4\pi} \int d^2\vec{r} B = \pm \frac{e}{2} \Phi ,$$

Each zero-energy state filled (unfilled) contributes $+1/2$ ($-1/2$) of an electron macroscopically: $(1/2) * \text{LL density}$

Some interesting graphene
facts:

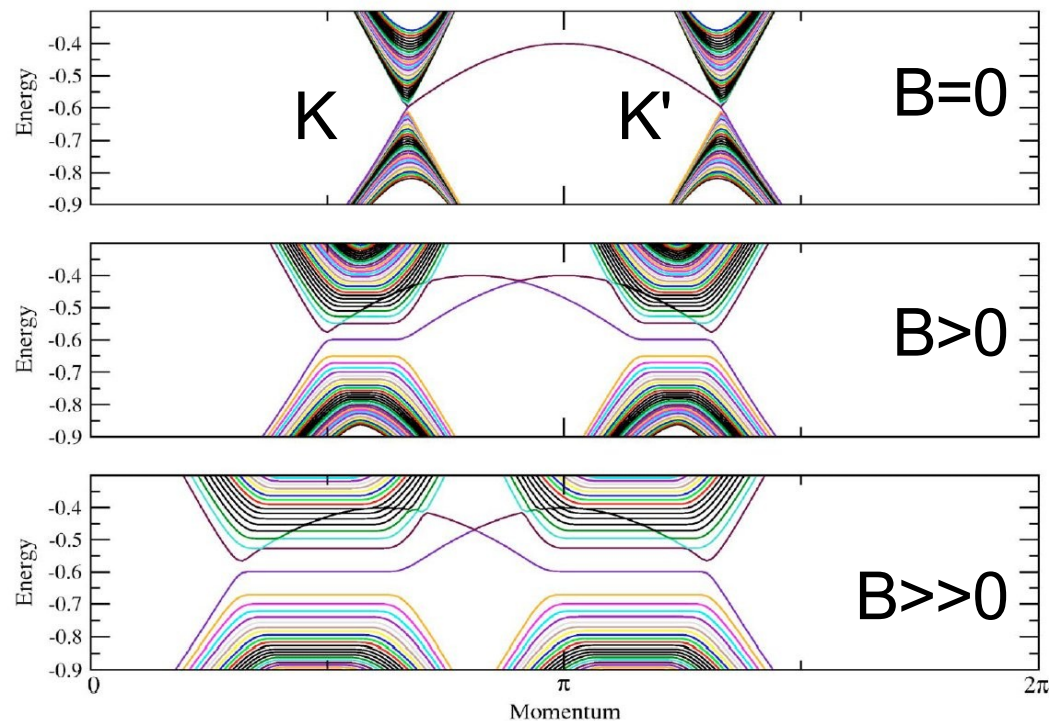
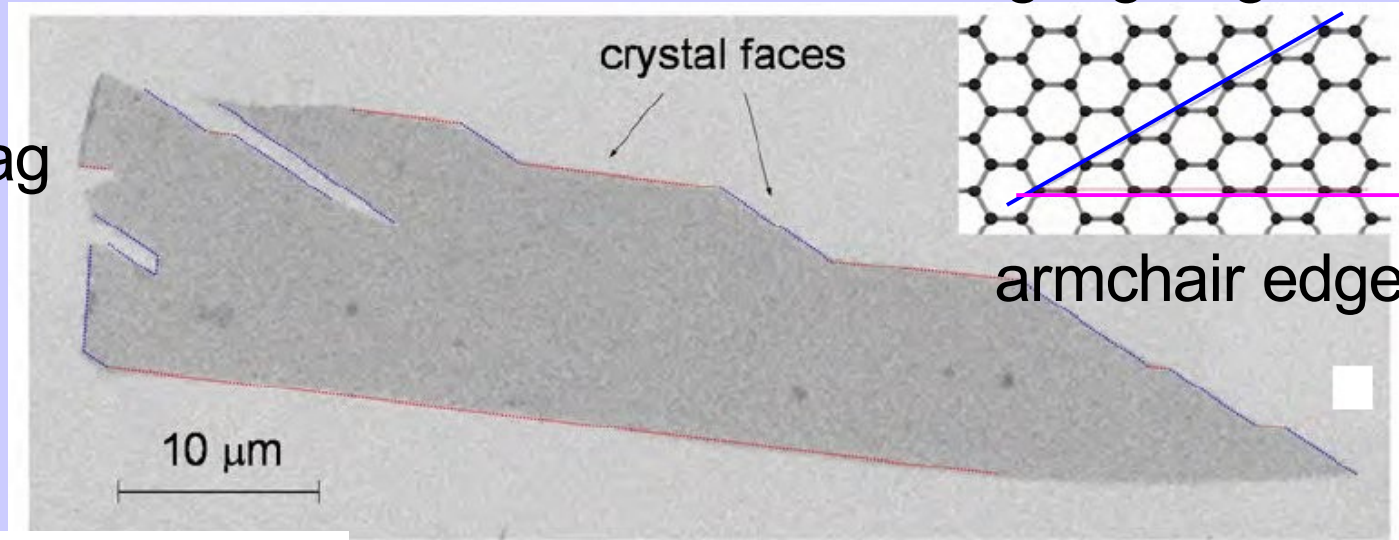
surface states at $B=0$;
QHE in bilayers;
valley-split and spin-split
QHE states

For zigzag edge surface states possible even without B field!

zigzag edge

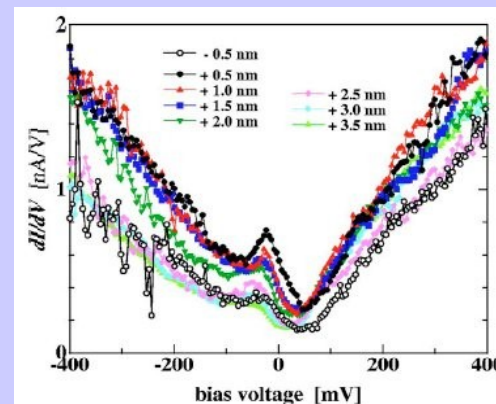
Surface mode propagating along zigzag edge (weak dispersion due to *nnn* coupling)

Momentum space:
(Peres, Guinea, Castro Neto)

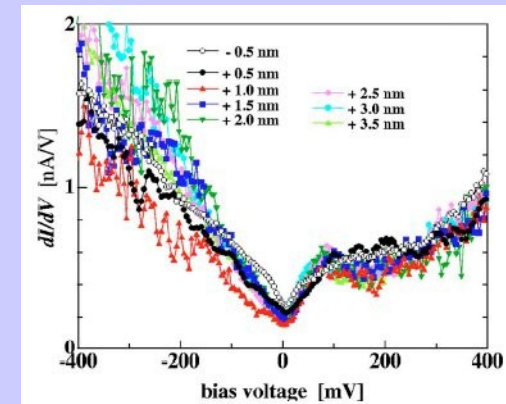


crystallites not just flakes

Scanning tunneling spectroscopy of 3D graphite top layer (Niimi et al 2006)

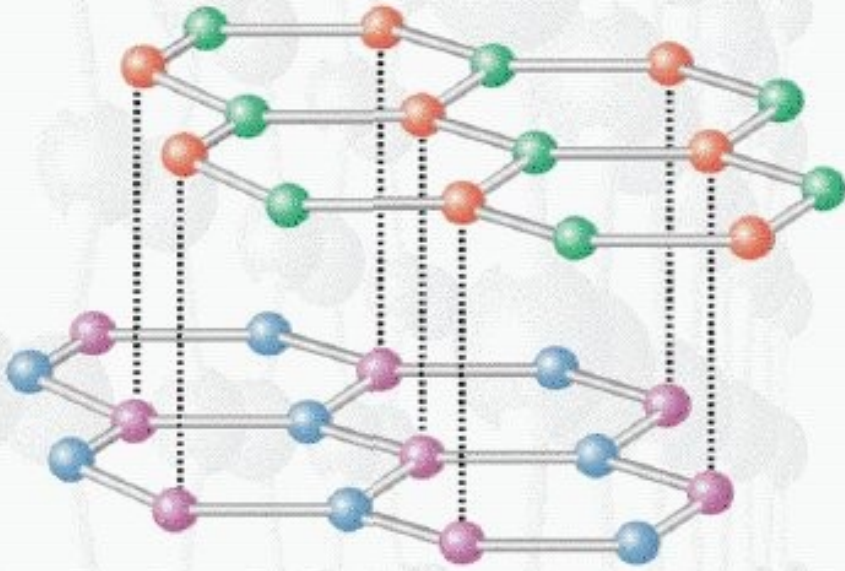


zigzag



armchair

Graphene bilayer: electronic structure and QHE

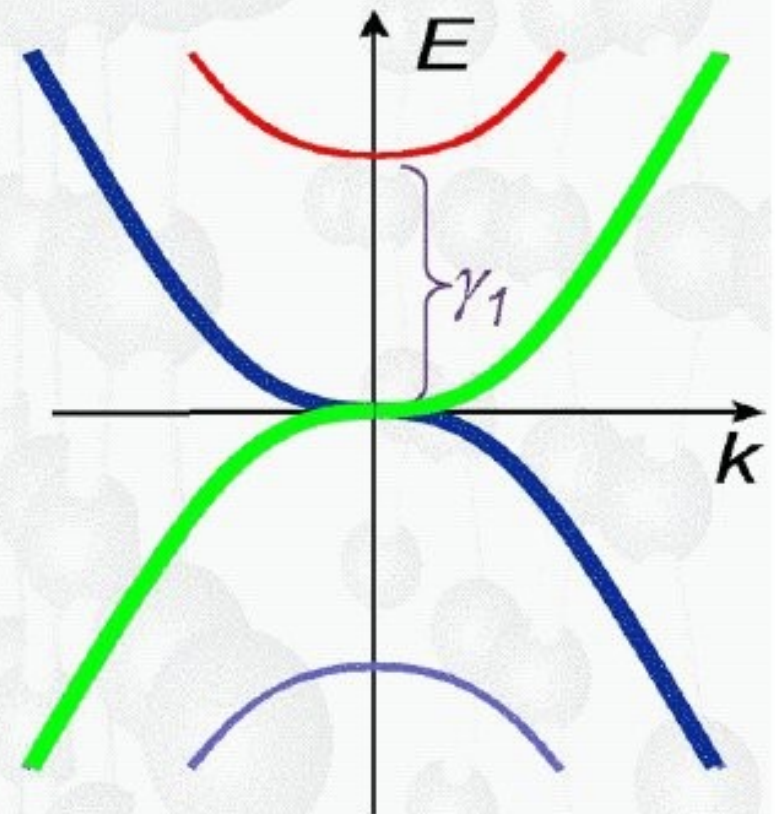


$$E(p) = \pm \frac{1}{2} \gamma_1 \pm \sqrt{\frac{1}{4} \gamma_1^2 + v_F^2 p^2}$$

$$\hat{H} = -\frac{1}{2m} \begin{pmatrix} 0 & (\hat{p}_x + i\hat{p}_y)^2 \\ (\hat{p}_x - i\hat{p}_y)^2 & 0 \end{pmatrix}$$

$$E_N = \pm \hbar \omega_c \sqrt{N(N-1)}$$

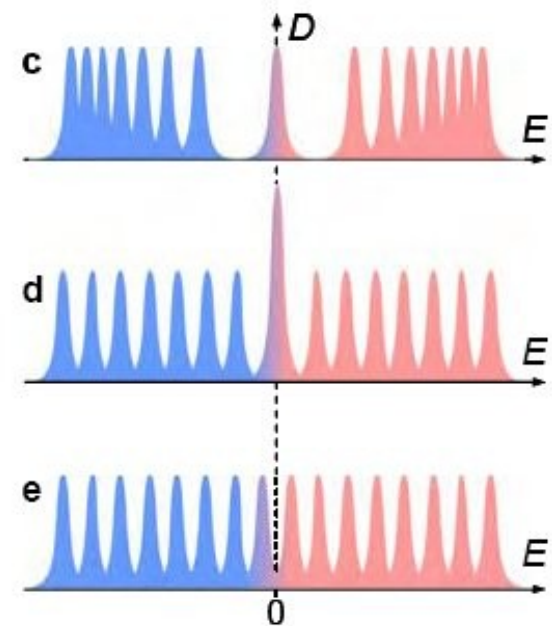
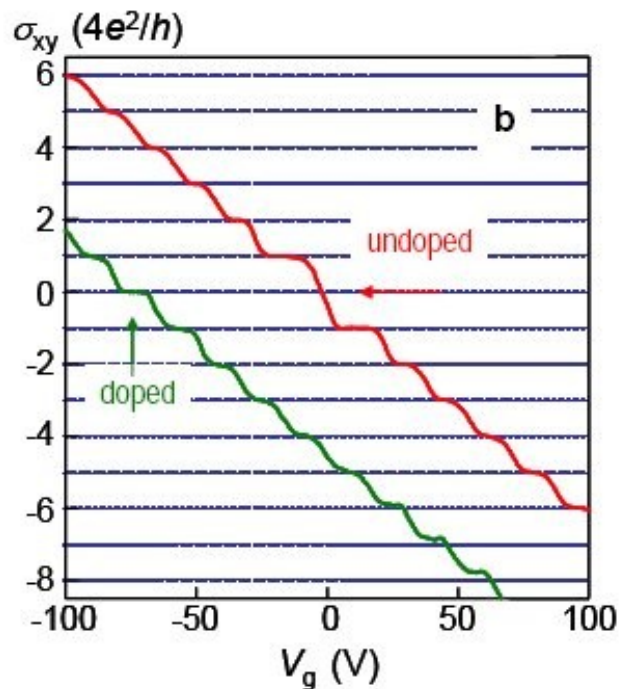
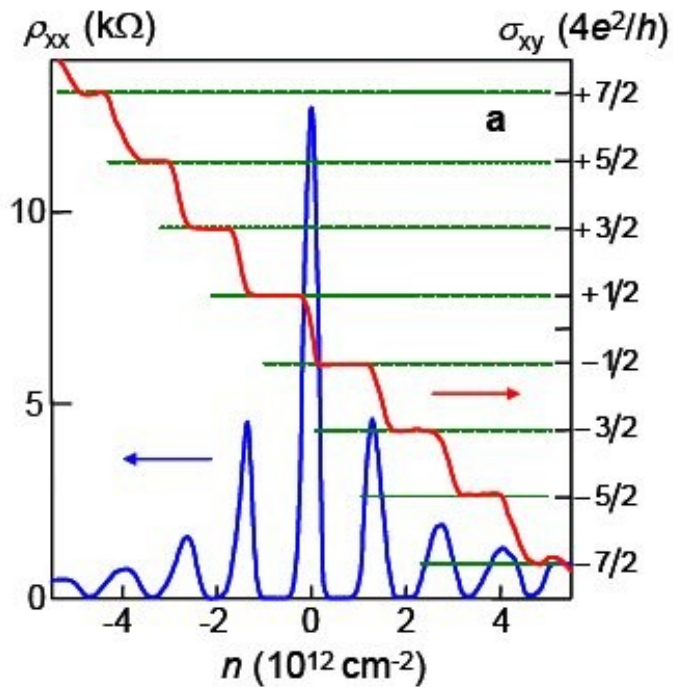
McCann & Falco 2006



Bilayer: field-tunable semiconducting energy gap

monolayer

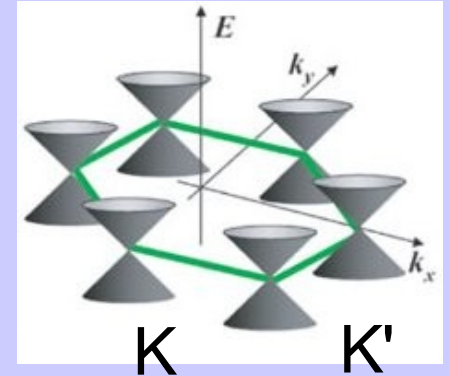
bilayer



Pseudospin $K-K'$ valley states

(i) Spin and valley $n=0$ Landau level degeneracy:

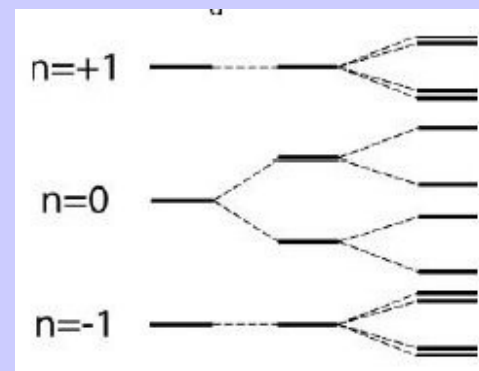
$$2 \times 2 = 4;$$



(ii) $SU(4)$ symmetry, partially lifted by Zeeman interaction:

$SU(4)$ lowered to $SU(2)$, associated with KK' mixing;

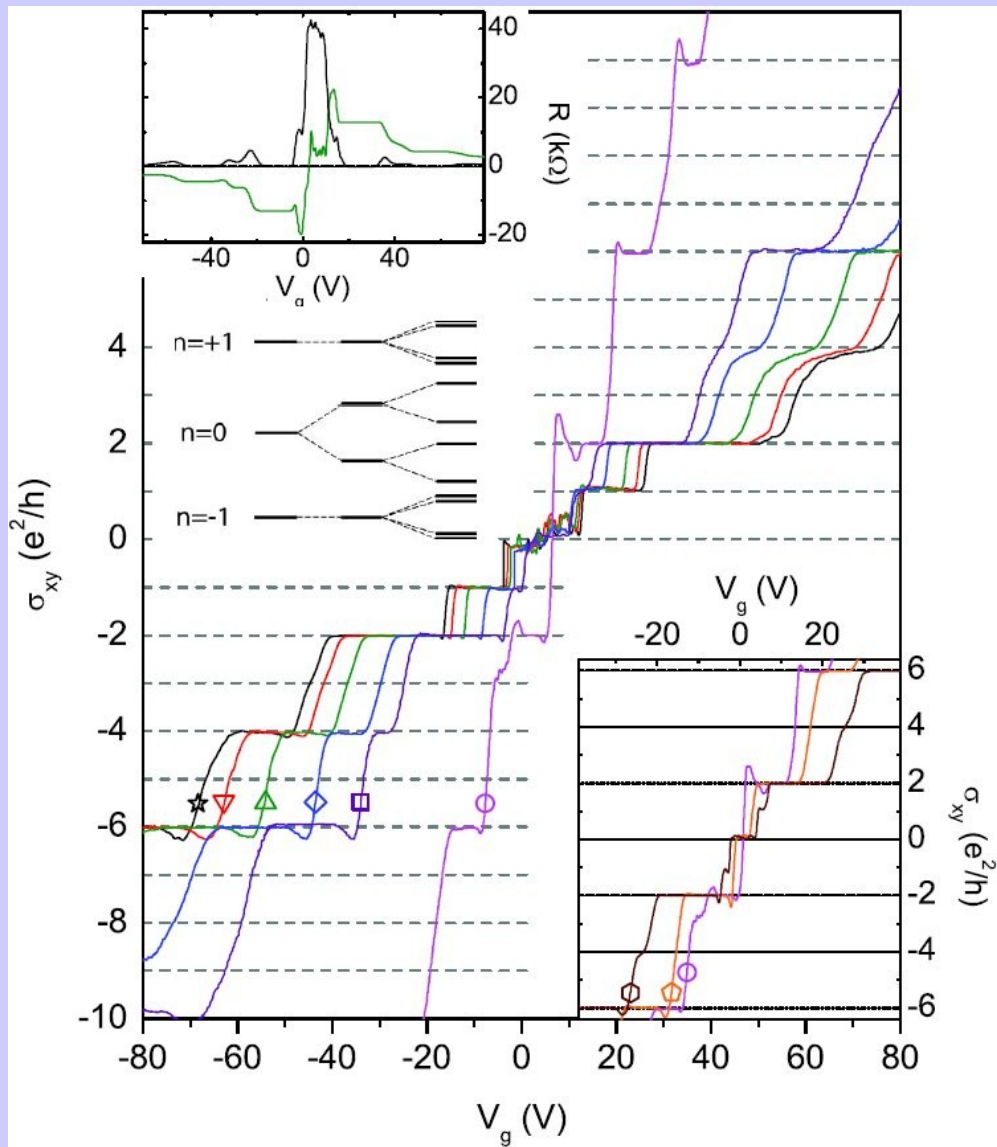
(iii) Assume that the $\nu=1$ QHE plateau is described by KK' splitting of spin-polarized $n=0$ Landau level



Many aspects similar to quantum Hall bi-layers (here KK')

Girvin, MacDonald 1995, and others

Observation of valley-split QHE states



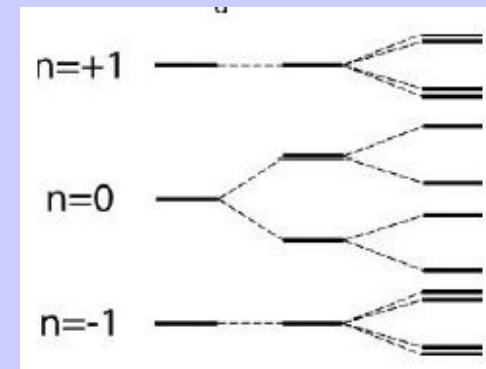
Four-fold degenerate $n=0$ LL splits into sub-levels at ultra high magnetic field:

spin ($n=0,+1,-1$), KK' ($n=0$)

confirmed by exp in tilted field 😊

$B=9,25,30,37,42,45$ Tesla, $T=1.4$ K

(Zhang et al, 2006)



HW?

Lecture III

QHE in p-n and p-n-p
lateral junctions:

Edge state mixing;
Fractionally-quantized QHE

Reviews on graphene:

Topical volume (collection of short reviews):
Solid State Comm. v.143 (2007)

A. Geim & K. Novoselov “The rise of graphene”
Nature Materials v.6, 183 (2007)

QHE in p-n junctions I

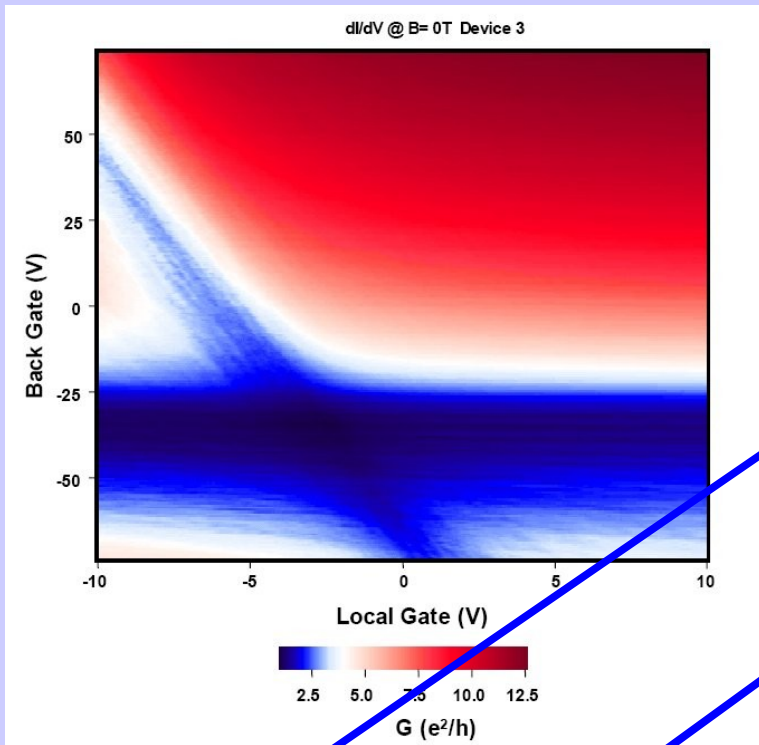
Local density control (gating): p-n and p-n-p junctions

(Stanford, Harvard, Columbia)

QHE in p-n junctions, integer and fractional conductance quantization:

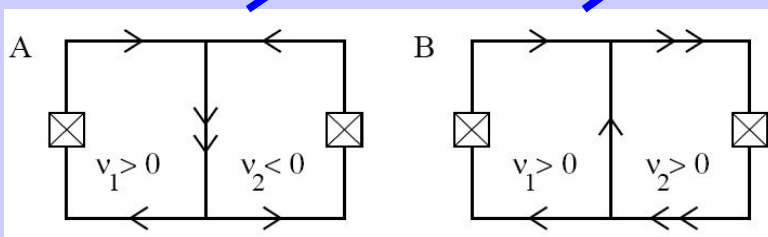
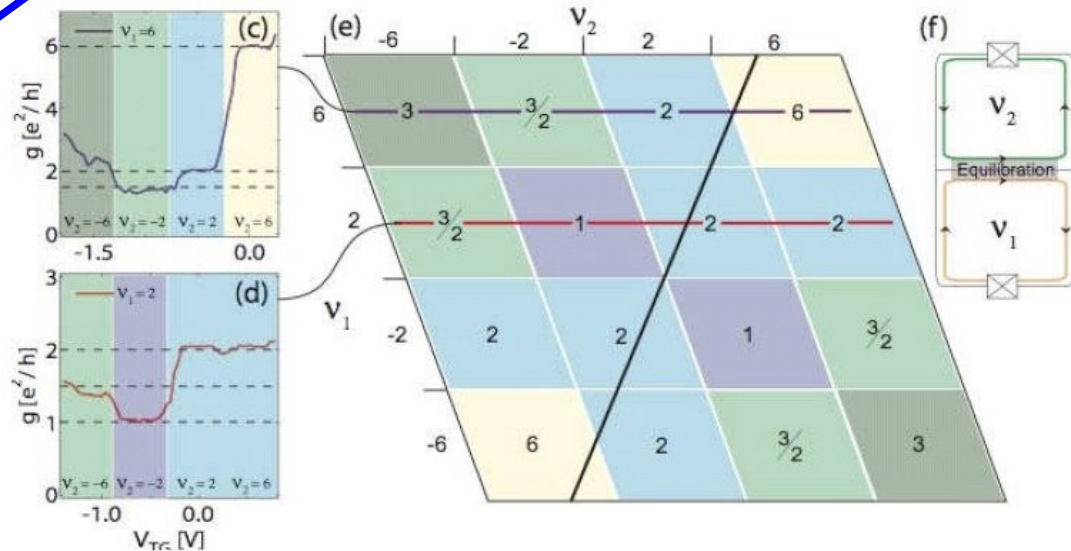
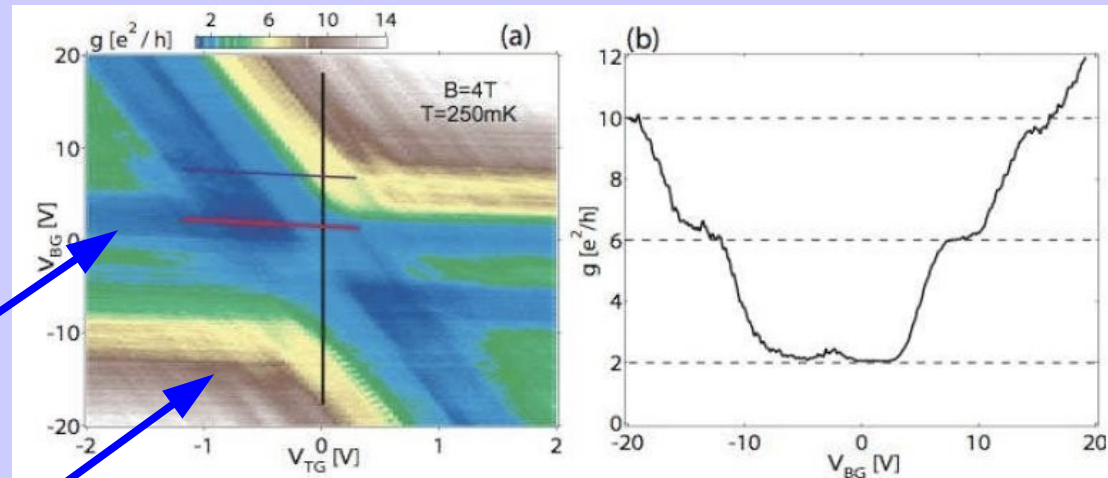
(i) $g=2,6,10\dots$, unipolar regime, (ii) $g=1,3/2\dots$, bipolar regime

Williams, DiCarlo, Marcus, Science 28 June 2007



$B > 0$

$B = 0$

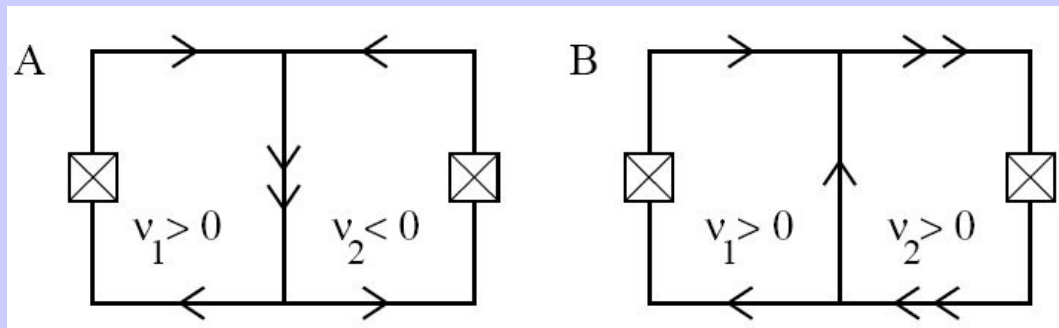


QHE in p-n junctions II

p-n

n-n, p-p

No mixing



$$g_{nn} = g_{pp} = \min(|\nu_1|, |\nu_2|) = 2, 6, 10, \dots$$

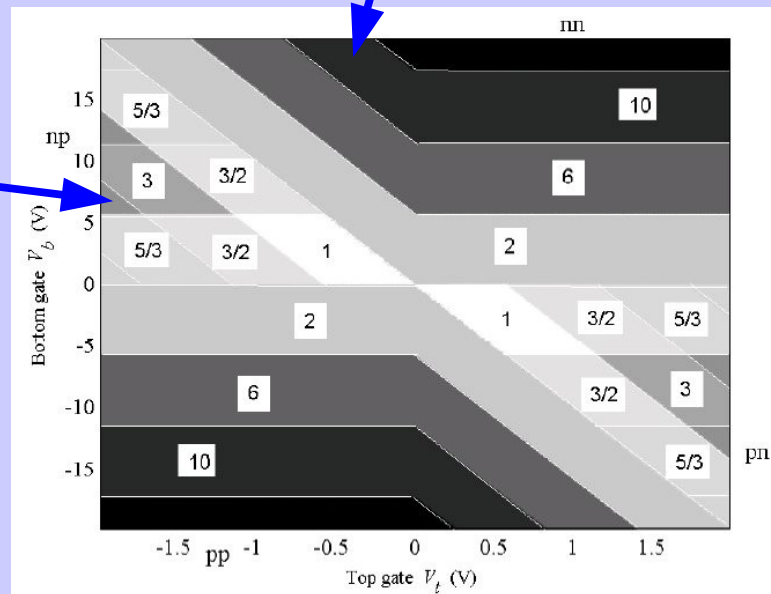
Noiseless transport

Mode mixing, but UCF suppressed

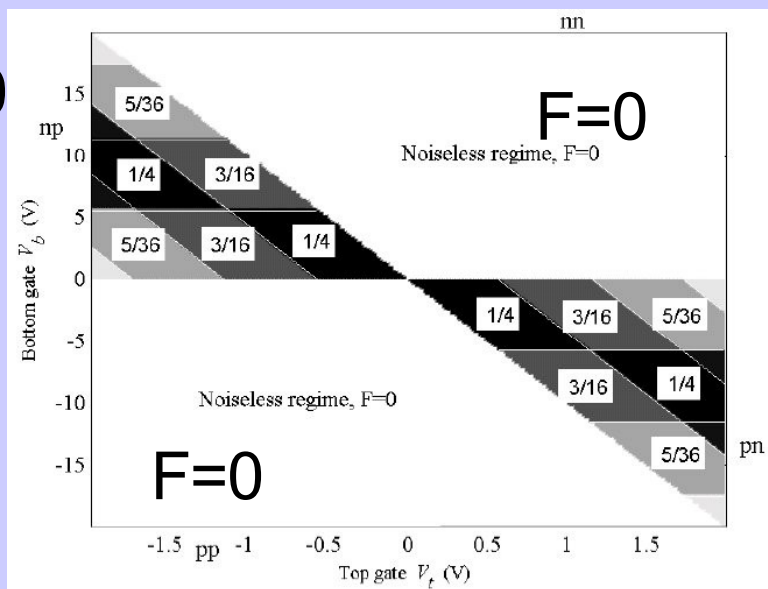
Quantized conductance

$$g_{pn} = \frac{|\nu_1||\nu_2|}{|\nu_1| + |\nu_2|} = 1, \frac{3}{2}, 3, \frac{5}{3}, \dots$$

Current partition, noise



F > 0



F > 0

Quantized shot noise (fractional F=S/I)

Edge states mixing and fractional QHE in p-n-p junctions

Ozyilmaz et al 2007

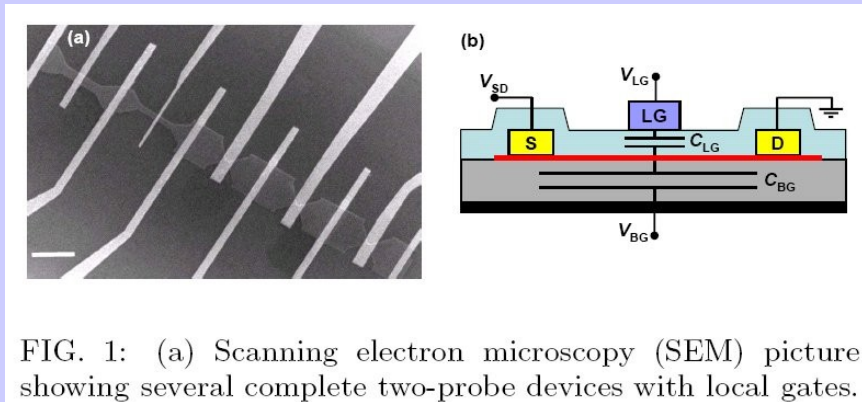
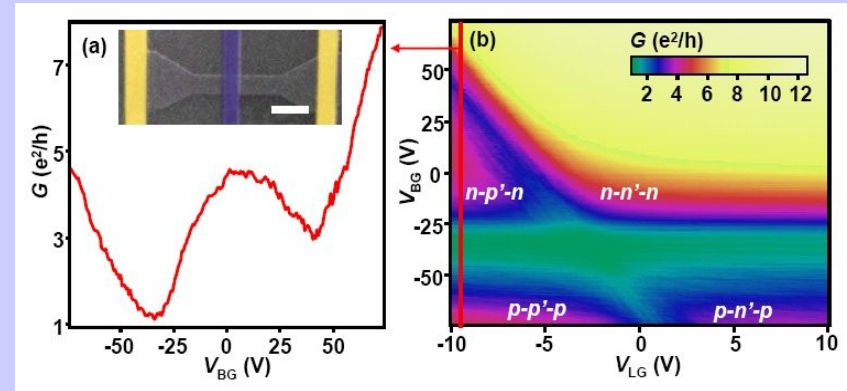
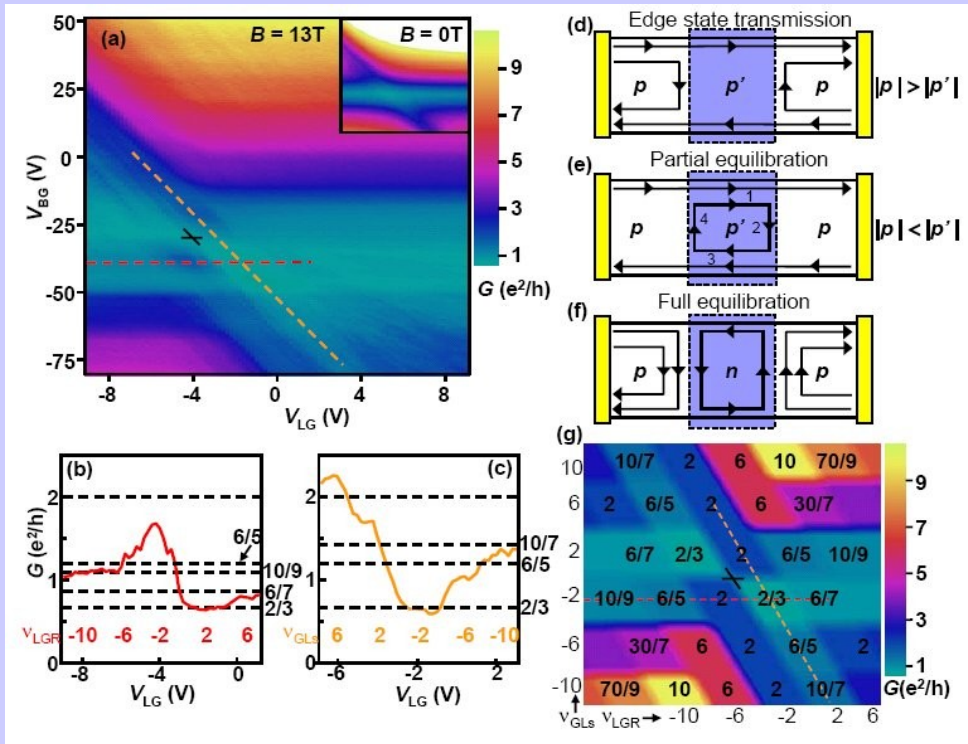


FIG. 1: (a) Scanning electron microscopy (SEM) picture showing several complete two-probe devices with local gates.

B=0



B>0



$$G = (e^2/h)|\nu'|, \quad |\nu'| \leq |\nu|$$

$$G = \frac{e^2}{h} \frac{|\nu'| |\nu|}{2|\nu'| - |\nu|} = \frac{6}{5}, \frac{10}{9}, \frac{30}{7}, \dots \quad (|\nu'| \geq |\nu|)$$

$$G = \frac{e^2}{h} \frac{|\nu'| |\nu|}{2|\nu'| + |\nu|} = \frac{2}{3}, \frac{6}{5}, \frac{6}{7}, \dots \quad (\nu\nu' < 0)$$

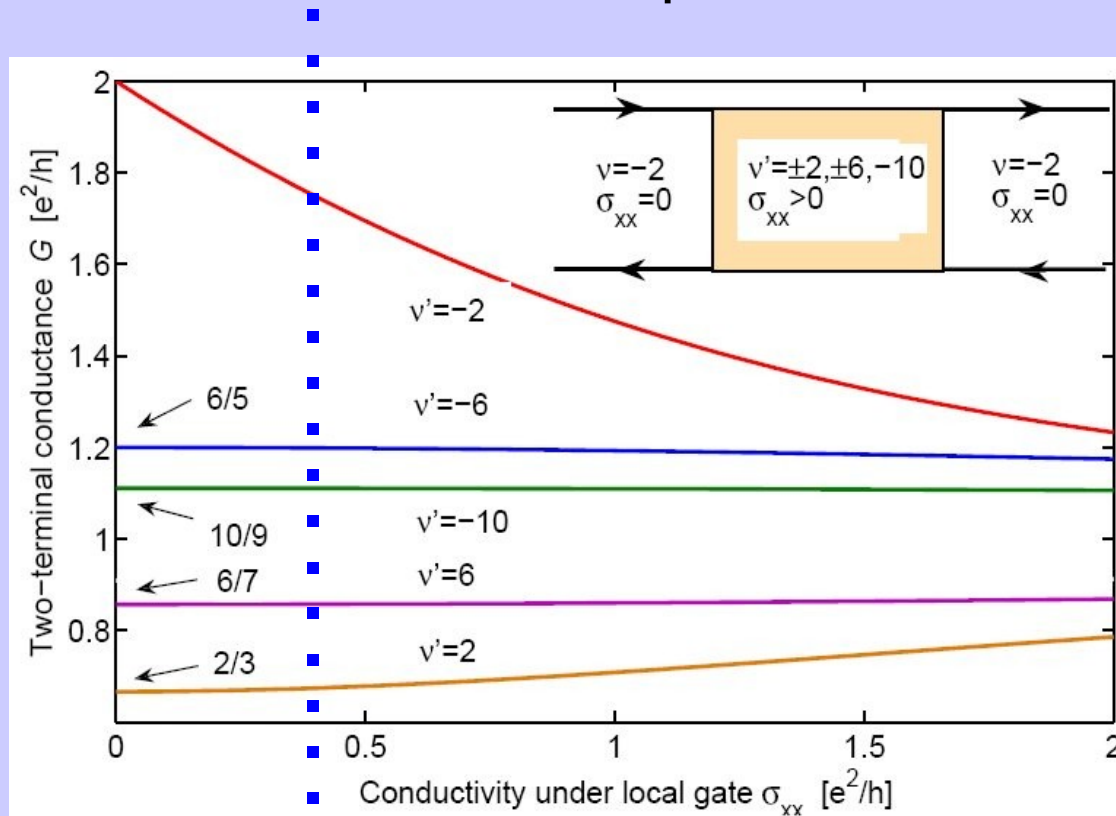
Little or no mesoscopic fluctuations

Stability of different fractional plateaus

2D transport vs 1D edge transport: results are identical at $\sigma_{xx}=0$

Model exactly solved by conformal mapping:
by generalizing the method of Rendell, Girvin, PRB 23, 6610 (1981)

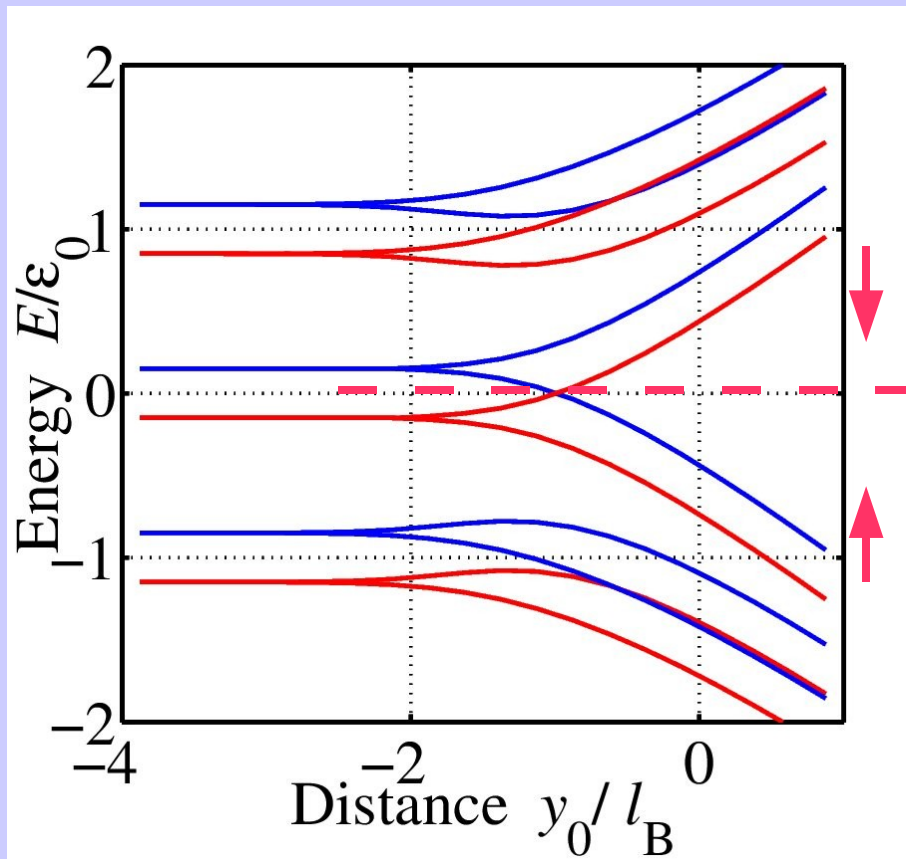
Plateaus with $\nu=\nu'$ less stable w.r.p.t. finite σ_{xx} than other plateaus



Spin transport at graphene edge

Abanin, P.A.Lee & LL PRL 96, 176803 (2006)

Spin-polarized edge states for Zeeman-split Landau levels



Near $\nu=0$, $E=0$:

- (i) Two chiral counter-propagating edge states;
- (ii) Opposite spin polarizations;
- (iii) No charge current, but finite spin current.

**Quantized spin Hall effect
(charge Hall vanishes)**

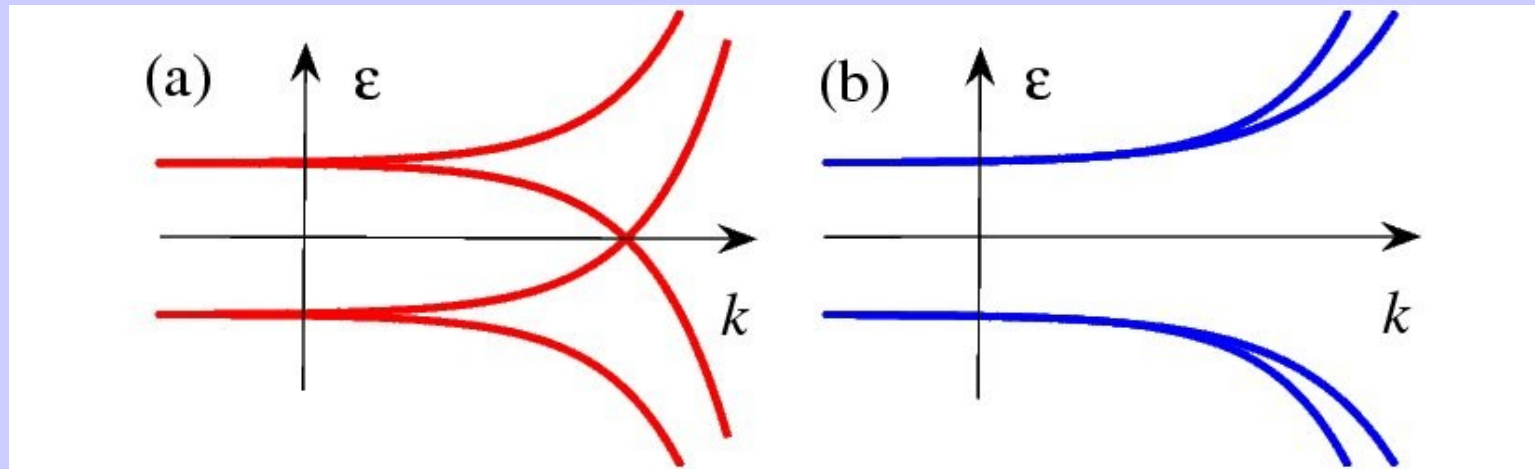
Edge transport as spin filter

Applications for spintronics

Similar to QSHE predicted by Kane and Mele (2005) in graphene with spin-orbital interaction ($B=0$, weak SO gap). Here a large gap!

What symmetry protects gapless edge states?

Gapless states, e.g. spin-split Gapped states, e.g. valley-split



Special Z_2 symmetry requirements (Fu, Kane, Mele, 2006):
in our case, the Z_2 invariant is S_z that commutes with H

Resembles massless Dirac excitations in band-inverted heterojunctions, such as PbTe, protected by supersymmetry (Volkov and Pankratov, 1985)

Manifestations in transport near the neutrality point

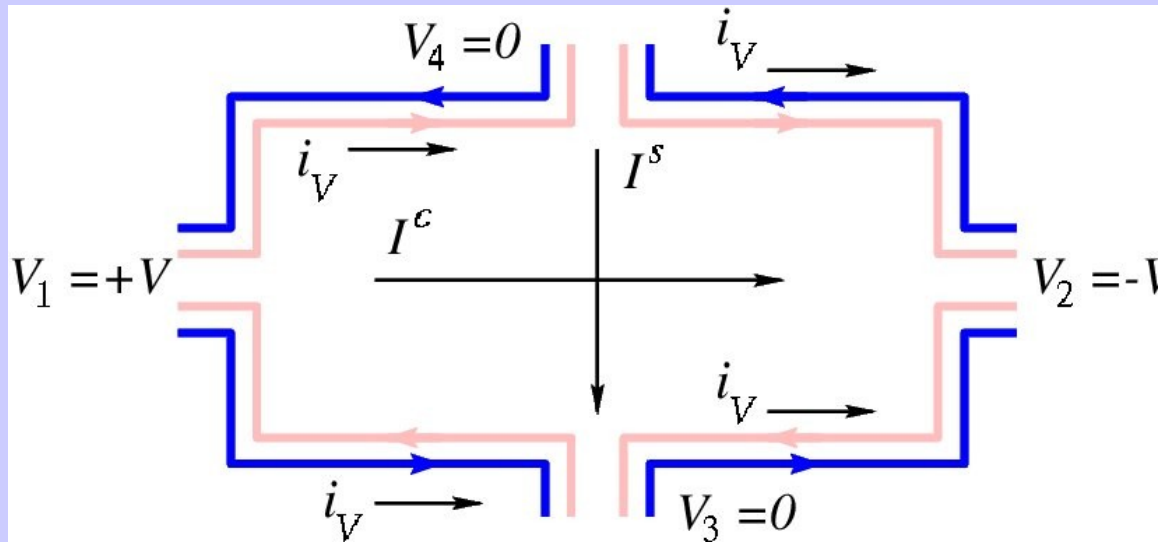
Gapless spin-polarized states:

- a) Longitudinal transport of 1d character;
- b) Conductance of order unity, e^2/h , at weak backscattering (SO-induced spin flips);
- c) No Hall effect at $\nu=0$

Gapped states:

- a) Transport dominated by bulk resistivity;
- b) Gap-activated temperature dependent resistivity;
- c) Hopping transport, insulator-like T-dependence
- d) Zero Hall plateau

Spintronics in graphene: chiral spin edge transport



Charge current

$$I_k^c = \sum_{k'} g_{kk'} (V_k - V_{k'})$$

(Landauer-Buttiker)

A 4-terminal device,
full spin mixing in contacts

Spin current
$$I_k^s = \sum_{k'} I_{kk'}^s = \sum_{k'} \epsilon_{kk'} g_{kk'} (V_k - V_{k'})$$

where $\epsilon_{kk'} = -\epsilon_{k'k}$ equals +1 (-1) when the current from k to k' is carried by spin up (spin down) electrons.

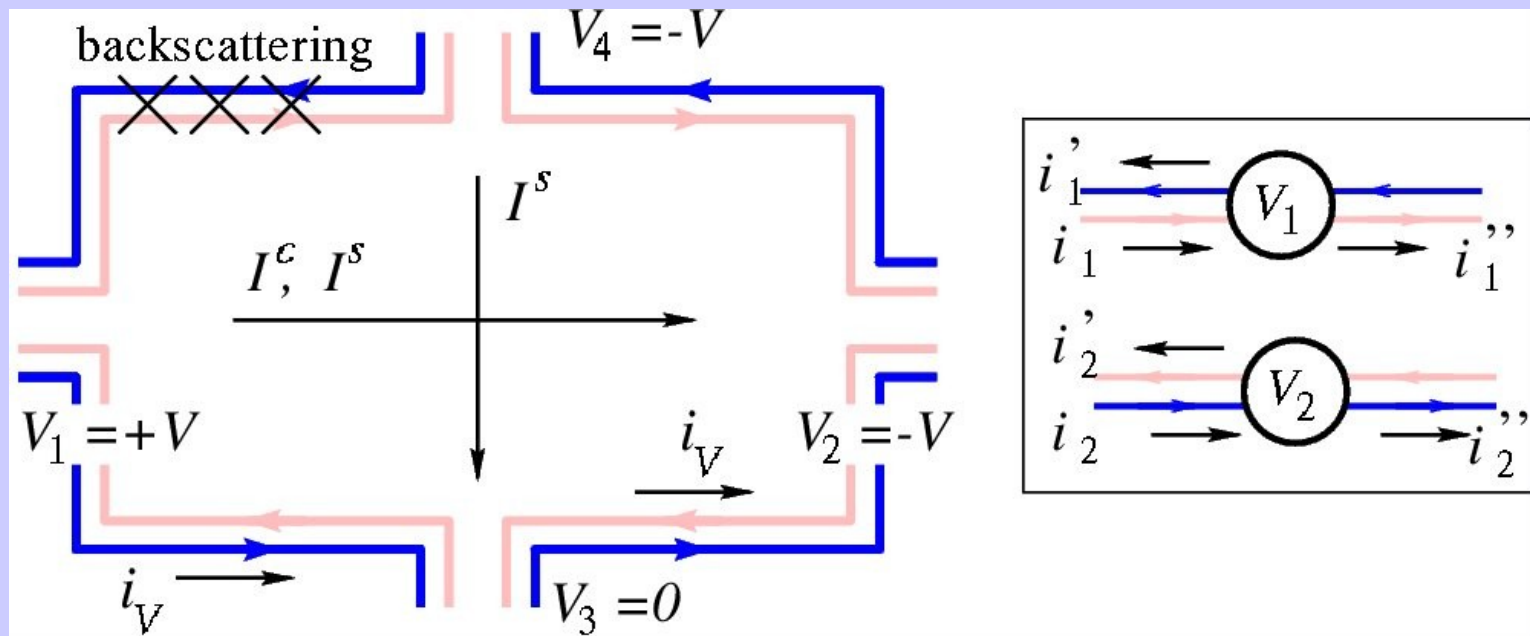
In an ideal clean system (no inter-edge spin-flip scattering):
charge current along V , spin current transverse to V :

$$\rho_{xx} = h/2e^2.$$

Quantized spin Hall conductance

Spin-filtered transport

Asymmetric backscattering filters one spin polarization, creates longitudinal spin current:



Hall voltage measures spin not charge current!

Applications: (i) spin injection; (ii) spin current detection.

Spin current without ferromagnetic contacts

Control spin-flip scattering?

- Rashba term very small, 0.5 mK;
- Intrinsic spin-orbit very small and also ineffective when spins are perpendicular to 2d plane;
- In-plane magnetic field tips the spins and allows to tune the spin-flip scattering, induce backscattering
- Magnetic impurities? Oxygen?

Applications for spintronics:

- 1) Quantized spin Hall effect (charge Hall effect vanishes);**
- 2) Edge transport as spin filter or spin source;**
- 3) Detection of spin current**

Estimate of the spin gap

Exchange in spin-degenerate LL's at $\nu=0$, $E=0$:

- Coulomb interaction favors spin polarization;
- Fully antisymmetric spatial many-electron wavefunction;
- Spin gap dominated by the exchange somewhat reduced by correlation energy:

$$\Delta = \frac{n}{2} \int \frac{e^2}{\epsilon r} \left(1 - e^{-r^2/2l_B^2}\right) d^2r = \left(\frac{\pi}{2}\right)^{1/2} \frac{e^2}{\epsilon l_B} (1 - \alpha)$$

correlation
↓

Gives spin gap $\sim 100\text{K}$ much larger than Zeeman energy (10K)

Chiral spin edge states summary

PRL 96, 176803 (2006) and PRL 98, 196806 (2007)

- ◆ Counter-propagating states with opposite spin polarization at $\mathbf{v}=\mathbf{0}$, $E=0$;
- ◆ Large spin gap dominated by Coulomb correlations and exchange
- ◆ Experimental evidence for edge transport: dissipative QHE near $\mathbf{v}=\mathbf{0}$ (see below)
- ◆ Gapless edge states at $\mathbf{v}=\mathbf{0}$ present a constraint for theoretical models
- ◆ Novel spin transport regimes at the edge (no experimental evidence yet)

Dissipative Quantum Hall effect

Abanin, Novoselov, Zeitler, P.A. Lee, Geim & LL,
PRL 98, 196806 (2007)

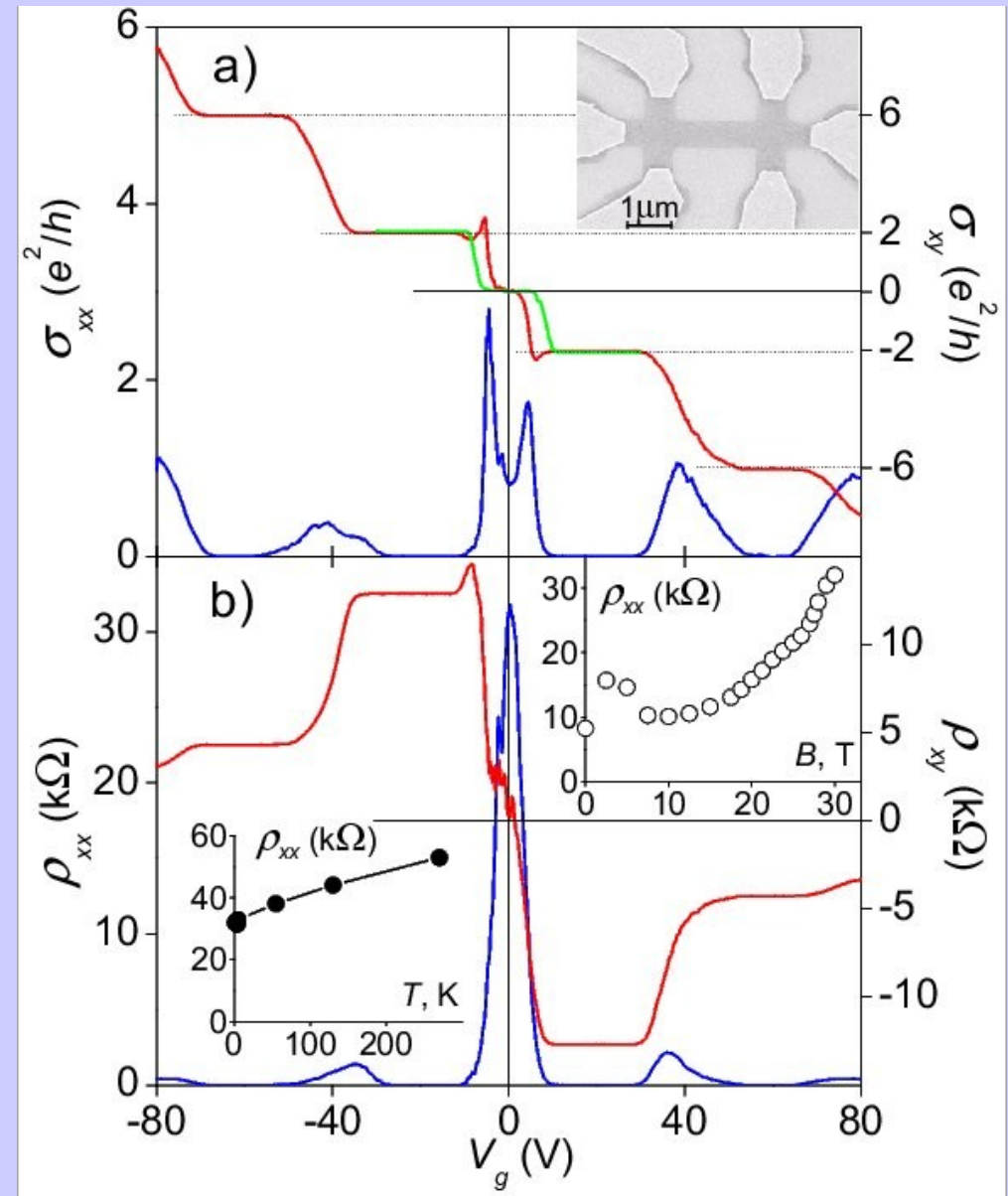
Dissipative QHE near $\nu=0$

Longitudinal and Hall resistance,
 $T=4\text{K}$, $B=30\text{T}$

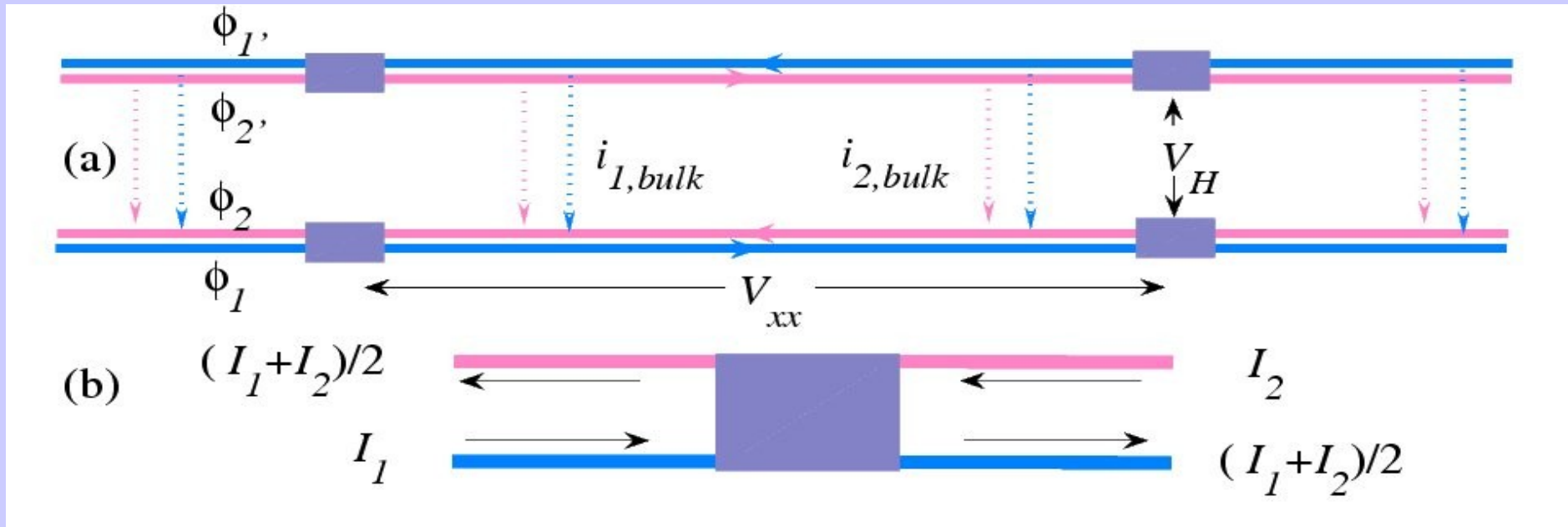
Features:

- a) Peak in ρ_{xx} with metallic T-dependence;
- b) Resistance at peak $\sim h/e^2$
- c) Smooth sign-changing ρ_{xy} no plateau;
- d) Quasi-plateau in calculated Hall conductivity, double peak in longitudinal conductivity

Novoselov, Geim et al, 2006



Edge transport model



$$I_1 = \frac{e^2}{h} \varphi_1, \quad I_2 = \frac{e^2}{h} \varphi_2, \quad I = I_1 - I_2$$

$$I_{1,2}^{(out)} = \frac{1}{2} (I_1 + I_2)$$

Ideal edge states, contacts with full spin mixing:
voltage drop along the edge across each contact
universal resistance value

$$V_{probe} = \frac{h}{e^2} I_{1,2}^{(out)}$$

Dissipative edge, unlike conventional QHE!

$$\Delta\varphi = \frac{h}{2e^2} (I_1 - I_2)$$

Backscattering (spin-flips), nonuniversal resistance
Estimate mean free path $\sim 0.5 \mu\text{m}$

$$R_{xx} = (\gamma L + 1) \frac{h}{2e^2}$$

Transport coefficients versus filling factor

Broadened, spin-split Landau levels

Bulk conductivity short-circuits edge:

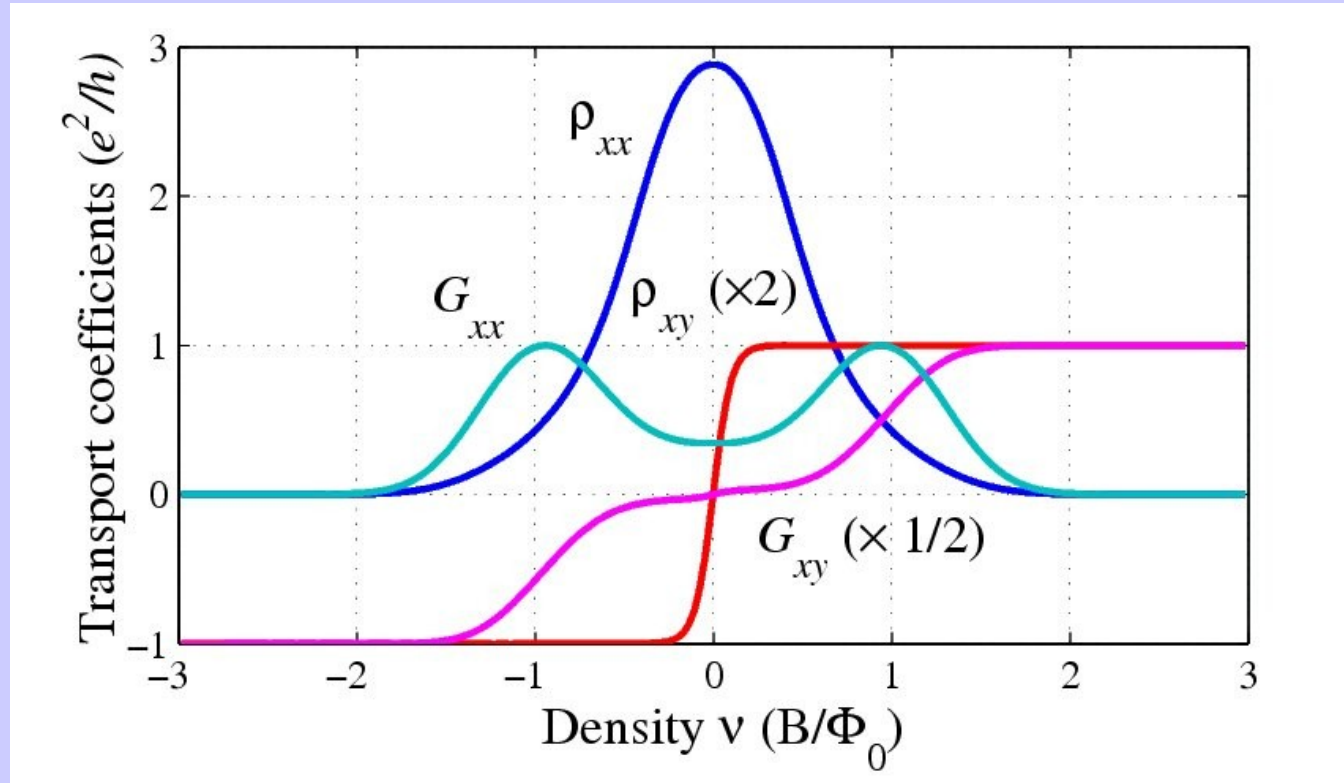
a) peak in ρ_{xx} at $\nu=0$;

b) smooth ρ_{xy} , sign change, no plateau

c) quasi-plateau in $G_{xy} = \rho_{xy} / (\rho_{xy}^2 + \rho_{xx}^2)$;

d) double peak in

$G_{xx} = \rho_{xx} / (\rho_{xy}^2 + \rho_{xx}^2)$



Model explains all general features of the data near $\nu=0$

The roles of bulk and edge transport interchange (cf. usual QHE): longitudinal resistivity due to edge transport, Hall resistivity due to bulk.

Charge impurities in graphene:

Atomic Collapse,
Dirac-Kepler scattering,
quasi-Rydberg states,
vacuum polarization,
screening

Shytov, Katsnelson & LL (2007)

Transport theory

Facts:

- linear dependence of conductivity vs. electron density;
- minimal conductivity $4e^2/h$

Born approximation:

$$\sigma = \frac{e^2}{\hbar} 2k_F \ell = \frac{e^2}{\hbar} 2E_F \tau_0 / \hbar, \quad \hbar / \tau_0 = 2\pi \nu_F \bar{V}^2$$

Charge impurities: dominant scattering mechanism (MacDonald, Ando)

$$V(q) = \frac{2\pi e^2}{\kappa(q + 4\alpha k_F)} \approx \frac{\hbar v \pi}{2k_F}, \quad \alpha = e^2 / \kappa \hbar v \approx 2.5$$

$$\sigma \propto (4e^2/h) n_{el} / n_{imp}$$

Screening of impurity potential: no difference on the RPA level

Effects outside Born and RPA approximation?

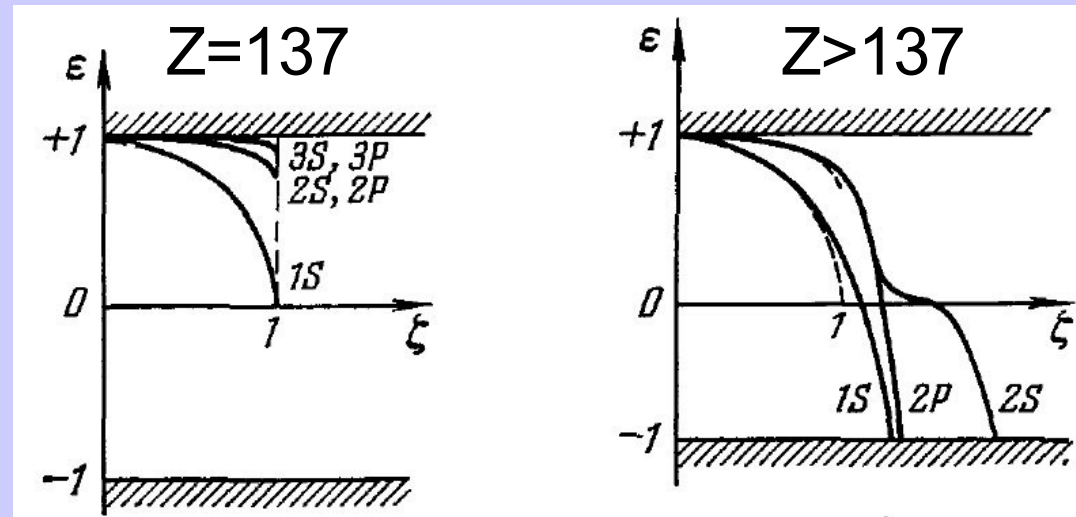
Anomaly in the Dirac theory of heavy atoms, $Z > 137$

Textbook solution for hydrogenic spectrum fails at $Z > 137$:

$$E_{n,j} = mc^2 \left[1 + \frac{(Z\alpha)^2}{(n - |\kappa| + \sqrt{\kappa^2 - (Z\alpha)^2})^2} \right]^{-1/2}, \quad \alpha \equiv \frac{e^2}{\hbar c} = \frac{1}{137}, \quad n, \kappa = 1, 2, 3, \dots$$

Finite nuclear radius important at $Z > 137$ (Pomeranchuk, Smorodinsky)

New spectrum at $137 < Z < 170$;
Levels diving one by one into the Dirac-Fermi sea at $Z > 170$
(Zeldovich, Popov, Migdal)



Quasiclassical interpretation:
collapsing trajectories in relativistic Kepler problem at $M < Ze^2/c$

The Dirac-Kepler problem in 2D

$$\hbar v_F \begin{pmatrix} 0 & -i\partial_x - \partial_y \\ -i\partial_x + \partial_y & 0 \end{pmatrix} \psi = \left(\varepsilon - \frac{\beta}{r} \right) \psi,$$

Potential strength

$$\beta \equiv -Ze^2/\hbar v_F.$$

In polar coordinates, angular momentum decomposition:

$$\psi(r, \varphi) = \begin{pmatrix} w(r) + v(r) \\ (w(r) - v(r)) e^{i\varphi} \end{pmatrix} r^{s-\frac{1}{2}} e^{im\varphi} e^{ikr}$$

$$s = \left((m + \frac{1}{2})^2 - \beta^2 \right)^{1/2}$$

Incoming and outgoing waves

For each m , a hypergeometric equation.

Different behavior: $|\beta| < |m + \frac{1}{2}|$, s real, $|\beta| > |m + \frac{1}{2}|$ s complex.

Scattering phases found from the relation

$$\frac{v}{w} = \exp \left(2ikr + 2i\beta \ln(2k\rho) - \pi i |m + \frac{1}{2}| + 2i\delta_m(k) \right)$$

Scattering phases

The phases δ_m are different in the subcritical and overcritical cases. For $|\beta| < |m + \frac{1}{2}|$,

$$\delta_m = \frac{\pi}{2}(|m + \frac{1}{2}| - s) - \arg \Gamma(s + 1 + i\beta) + \frac{1}{2} \arctan \frac{\beta}{s},$$

while for $|\beta| > |m + \frac{1}{2}|$ the scattering phase is given by

$$e^{2i\delta_m(k)} = e^{\pi i|m+\frac{1}{2}|} \frac{g_{\beta,\gamma} + e^{i\chi(k)} e^{-\pi\gamma} \eta g_{\beta,-\gamma}}{e^{-\pi\gamma} \eta g_{\beta,-\gamma}^* + e^{i\chi(k)} g_{\beta,\gamma}^*},$$

$$\chi(k) = 2\gamma \ln 2kr_0 + 2 \tan^{-1} \frac{1+\eta}{1-\eta}, \quad \eta \equiv \sqrt{\frac{\beta-\gamma}{\beta+\gamma}},$$

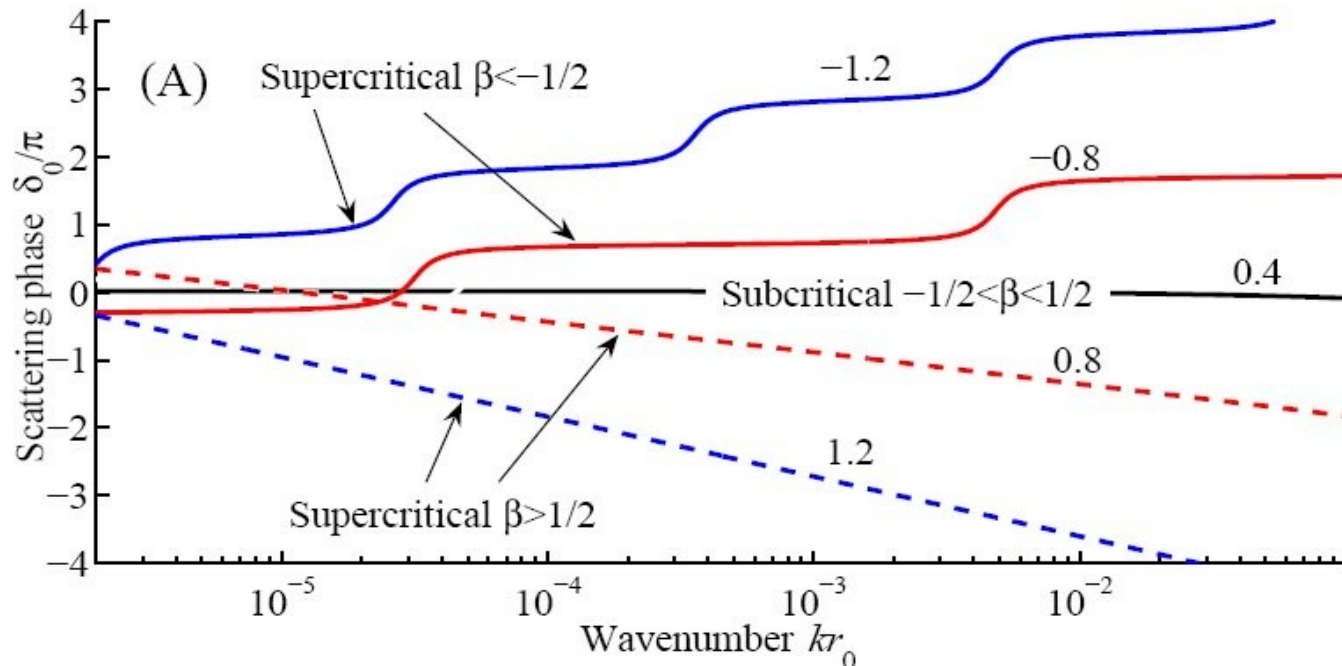
where $\gamma \equiv \sqrt{\beta^2 - (m + \frac{1}{2})^2}$ and $g_{\beta,\gamma} \equiv \frac{\Gamma(1+2i\gamma)}{\Gamma(1+i\gamma+i\beta)}$.

Subcritical potential strength

Supercritical potential strength.
Use boundary condition on lattice scale $r=r_0$

Subcritical δ 's
energy-independent

Supercritical δ 's
depend on energy,
 π -kinks or no π -kinks



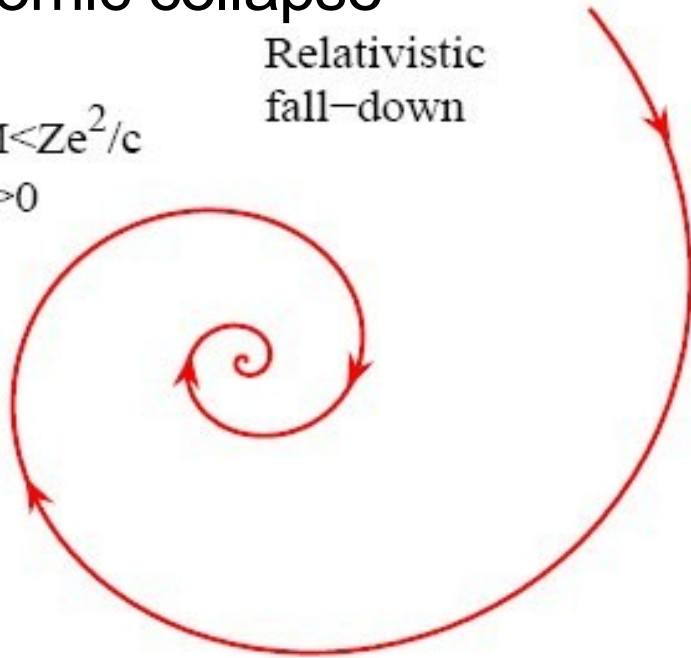
Quasistationary states I

Atomic collapse

$$M < Ze^2/c$$

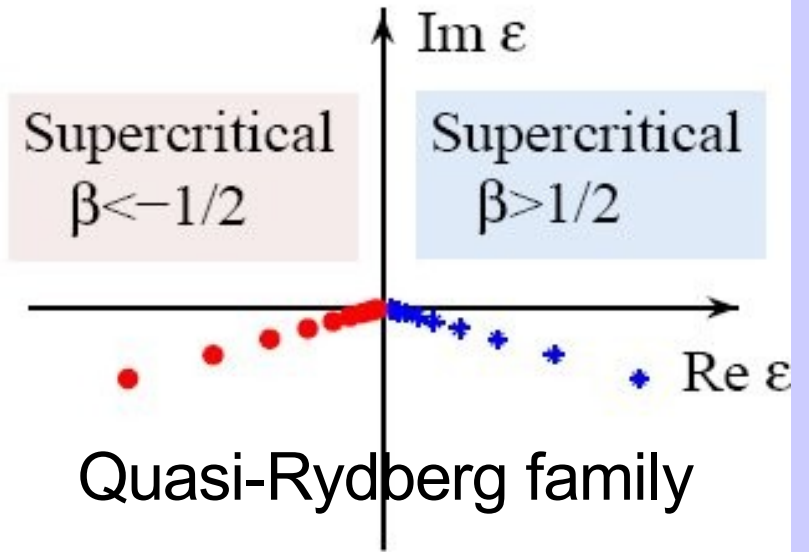
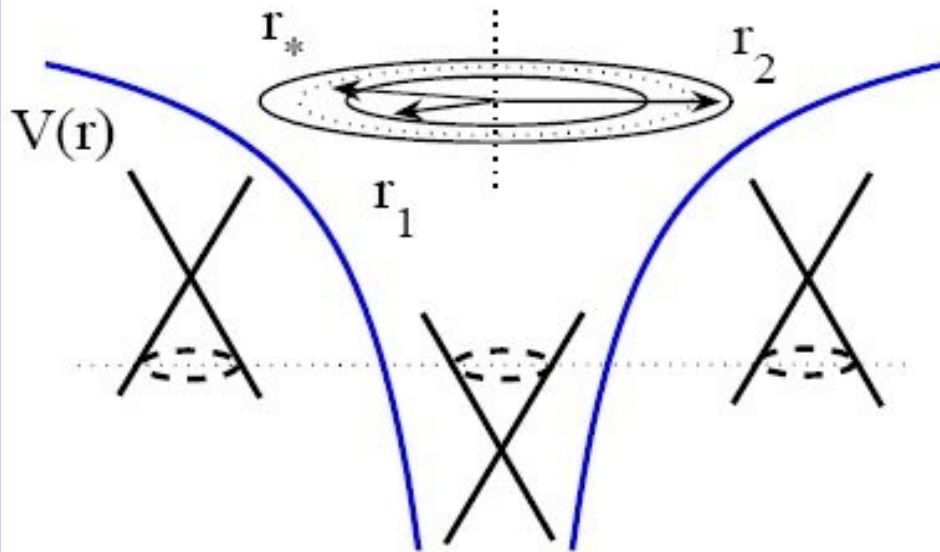
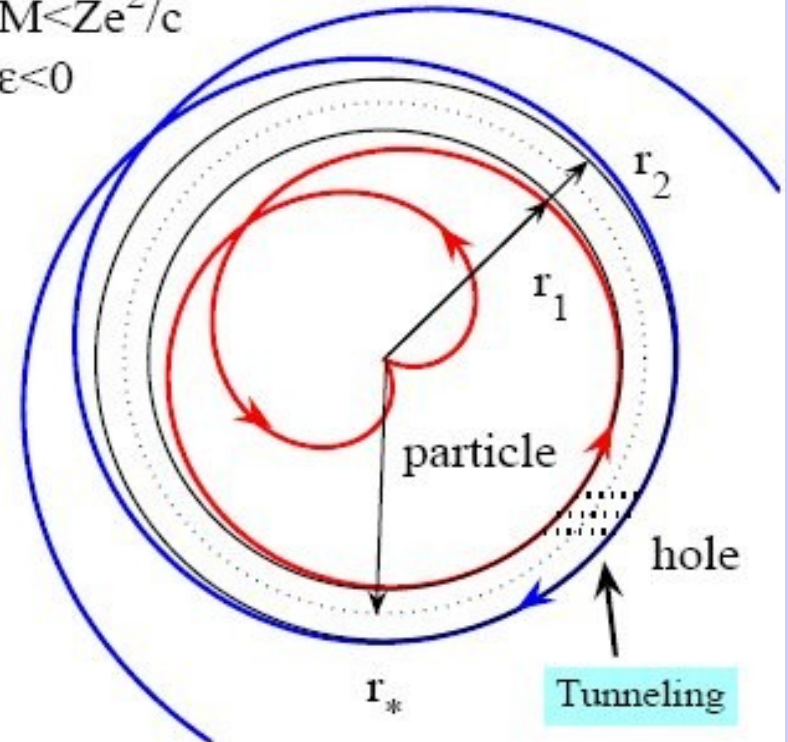
$$\epsilon > 0$$

Relativistic
fall-down



$$M < Ze^2/c$$

$$\epsilon < 0$$



Quasistationary states II

$$p_r^2 = v_F^{-2} \left(\varepsilon + \frac{Ze^2}{r} \right)^2 - \frac{M^2}{r^2}, \quad M < M_c = Ze^2/v_F$$

Classically forbidden region
Bohr-Sommerfeld condition:

$$r_1 < r < r_2$$

$$r_{1,2} = (Ze^2 \mp Mv_F)/\varepsilon.$$

$$\int_{r_0}^{r_1} p_r dr = \pi \hbar n, \quad \varepsilon_n \approx \frac{Ze^2}{r_0} e^{-\pi \hbar n / \gamma}, \quad n > 0$$

Resonance width:

lattice scale

$$\gamma \equiv (M_c^2 - M^2)^{1/2}$$

$$\Gamma_n \approx e^{-2S/\hbar} \sim |\varepsilon_n| \exp(-2\pi Ze^2/\hbar v_F)$$

$$S = \int_{r_1}^{r_2} dr \sqrt{\frac{M^2}{r^2} - \left(\frac{\varepsilon}{v_F} + \frac{M_c}{r} \right)^2} = \pi (M_c - \gamma)$$

Transport cross-section

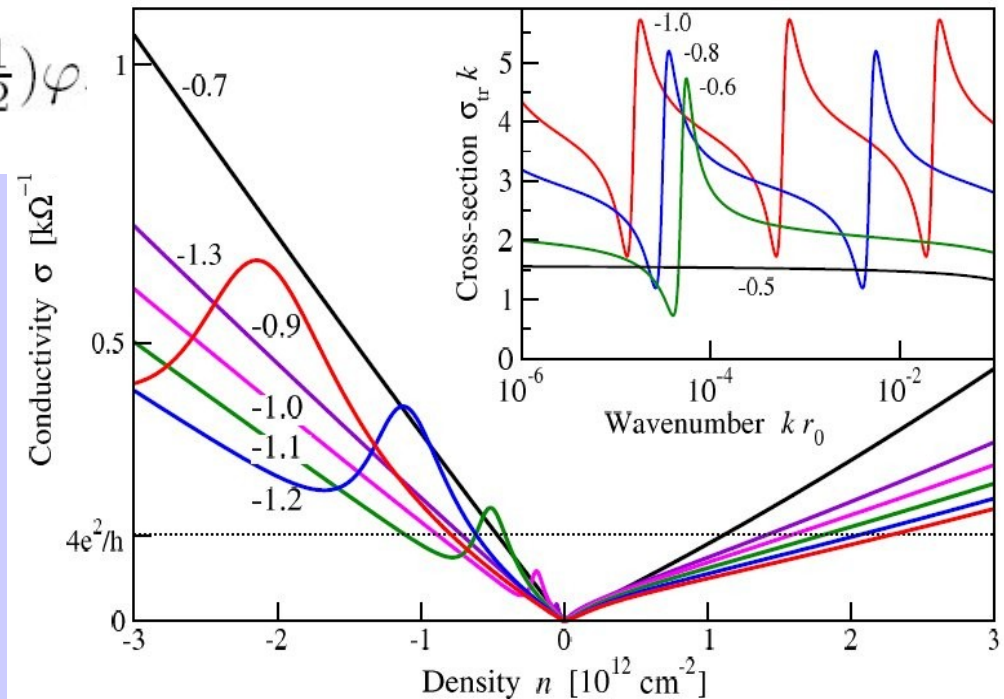
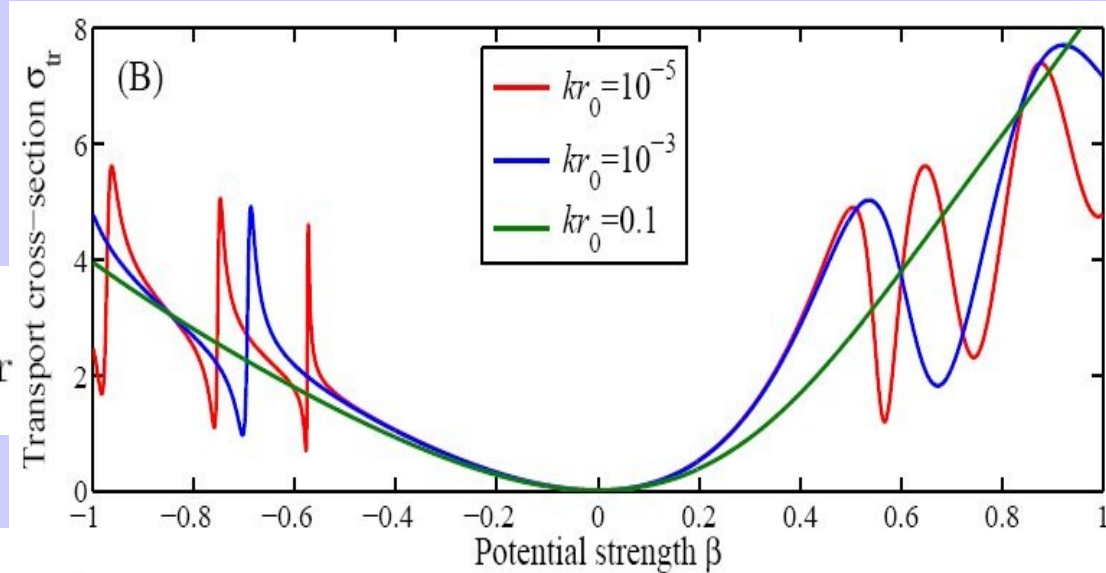
Drude conductivity

$$\sigma = \frac{e^2}{h} 2E_F \tau, \quad \tau^{-1} = v_F n_{\text{imp}} \sigma_{\text{tr}}$$

$$\sigma_{\text{tr}} = \int d\varphi (1 - \cos \varphi) |f(\varphi)|^2 = \frac{4}{k} \sum_{m=0}^{\infty} \sin^2(\delta_m - \delta_{m+1})$$

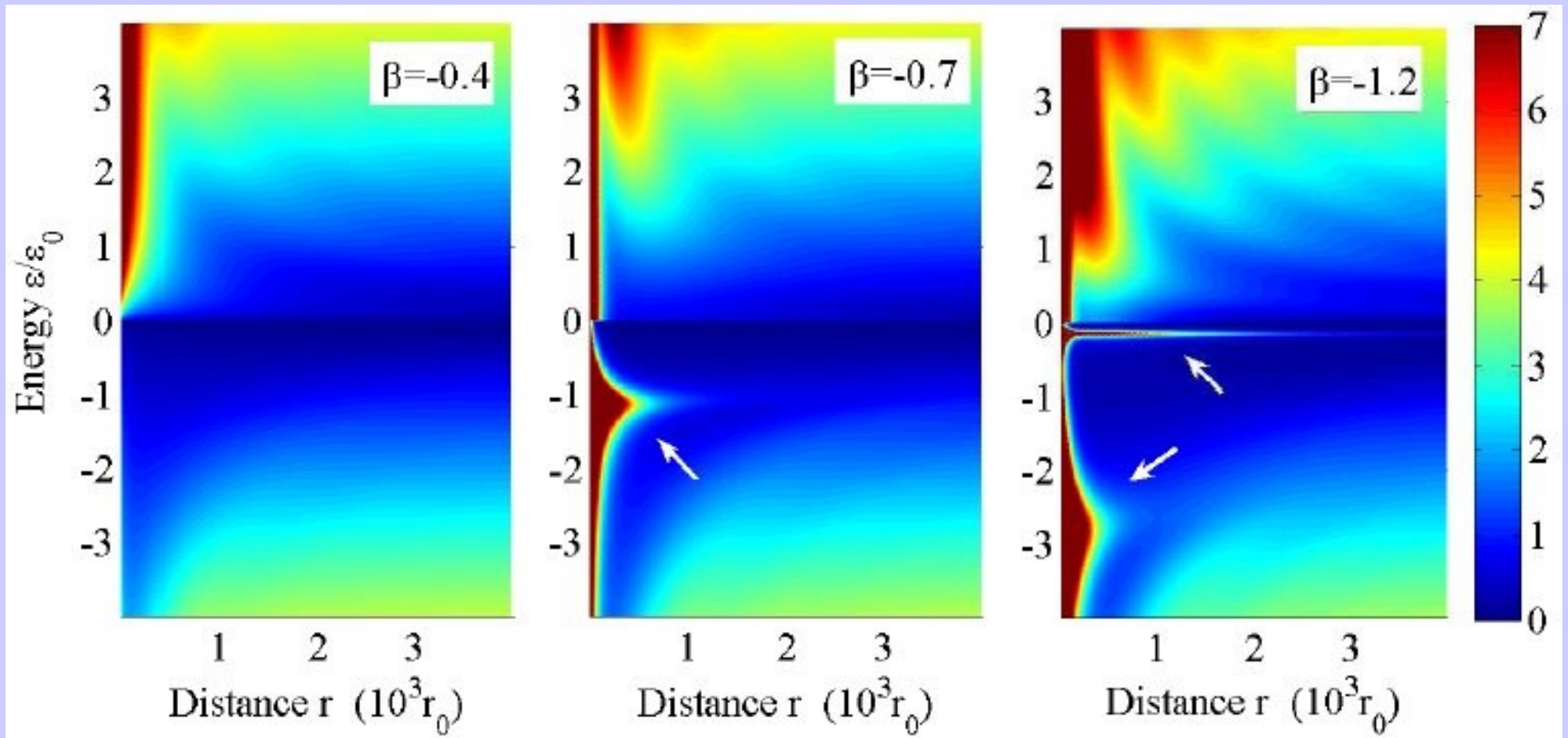
$$f(\varphi) = \frac{2i}{\sqrt{2\pi ik}} \sum_{m=0}^{\infty} (e^{2i\delta_m} - 1) \cos\left(m + \frac{1}{2}\right)\varphi$$

Resonance peaks when Fermi level aligns with one of quasiRydberg states



Resonances in the local density of states (LDOS)

Tunneling spectroscopy



Energy scales as the width Γ and as $1/(\text{localization radius})$

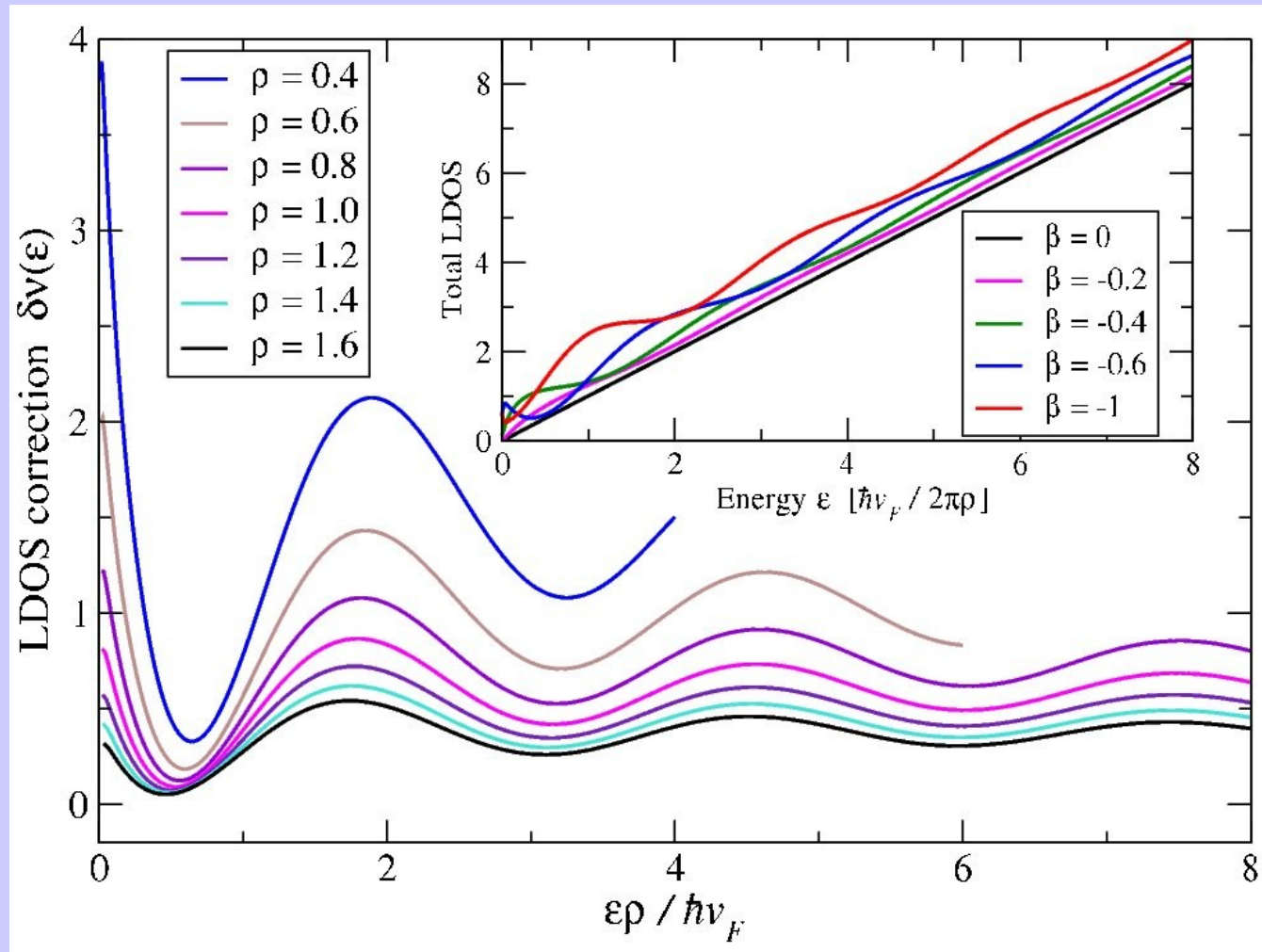
Oscillations in LDOS

Standing waves
(not Friedel oscillations)

for overcritical Coulomb
potential

period = $1/\text{energy}$

period > lattice constant,
can be probed with STM



Screening by massless Dirac particles: vacuum polarization

Critical Coulomb potentials in d=2:

$$\beta = \beta_c = \frac{1}{2}, \quad \beta \equiv \frac{Ze^2}{\kappa \hbar v_F}$$

$$Z_c \approx 1$$

In graphene:

$$\frac{e^2}{\hbar v_F} \approx 2.5$$

$$\kappa_{\text{RPA}} \approx 5.$$

Easier to realize than $Z > 137$ for heavy atoms!
Need divalent or trivalent impurities

$$\beta < \frac{1}{2}$$

Polarization charge localized on a lattice scale at

Mirlin et al (RPA), Sachdev et al (CFT)

A power law for overcritical potential:

$$n_{\text{pol}}(\rho) \approx -\frac{N\gamma \text{sign} \beta}{2\pi^2 \rho^2} + q_0 \delta(\rho), \quad \gamma \equiv \sqrt{\beta^2 - \frac{1}{4}}$$

$$\frac{1}{2} < \beta < \frac{3}{2}$$

Friedel sum rule argument

Use scattering phase to evaluate polarization?

Caution: energy and radius dependence for Coulomb scattering

$$\beta < \beta_c : \quad \theta(k) \approx \beta \ln k\rho$$

$$\beta > \beta_c : \quad \theta(k) \approx \beta \ln k\rho - \gamma \text{sign } \beta \ln kr_0$$

Geometric part, not related to scattering,
(deformed plane wave)

The essential part

$$Q_{\text{pol}}(\rho) = -N \frac{\theta(k \sim 1/\rho)}{\pi} = -\text{sign } \beta \frac{\gamma N}{\pi} \ln \frac{\rho}{2r_0}.$$

RG for polarization cloud

Log-divergence of polarization, negative sign,
but no overscreening!

RG flow of the net charge (source+polarization):

$$\frac{d\beta(\rho)}{d \ln \rho} = -\frac{N \operatorname{sign} \beta}{\pi \kappa} \gamma(\rho), \quad \beta > \beta_c.$$

Polarization cloud radius:

$$\rho_* = r_0 \exp\left(\frac{\pi \kappa}{N} \cosh^{-1}(2\beta)\right)$$

Nonlinear screening of the charge in excess of 1/2

Summary

- Different behavior for subcritical and supercritical impurities
- QuasiRydberg states in the supercritical regime
- Quasilocalized states (resonances), and long-period standing wave oscillations in LDOS around supercritical impurities
- No polarization away from impurity for charge below critical (in agreement with RPA)
- Power law $1/r^2$ for polarization around an supercritical charge
- Log-divergence of the screening charge: nonlinear screening of the excess charge $Q-1/2$, spatial structure described by RG

Atomic collapse, $Z > 170$, can be modeled by divalent or trivalent impurities in graphene

The End